# Kir2.1 Interactome Mapping Uncovers PKP4 as a Modulator of the Kir2.1-Regulated Inward Rectifier Potassium Currents


## Authors

Sung-Soo Park, Daniela Ponce-Balbuena, Rork Kuick, Guadalupe Guerrero-Serna, Justin Yoon, Dattatreya Mellacheruvu, Kevin P. Conlon, Venkatesha Basrur, Alexey I. Nesvizhskii, José Jalife, and Jean-François Rual

## Correspondence

jrual@umich.edu;
jjalife@umich.edu


## In Brief


A comprehensive map of the Kir2.1 interactome was generated using the proximity-labeling approach BioID. The map encompasses 218 interactions, the vast majority of which are novel, and explores the variations in the interactome profiles of Kir2.1$^{WT}$ versus Kir2.1$^{\Delta 314\text{-}315}$, a trafficking deficient ATS1 mutant, thus uncovering molecular mechanisms whose malfunctions may underlie ATS1 disease. PKP4, one of the BioID interactors, is validated as a modulator of Kir2.1-controlled inward rectifier potassium currents.


## Graphical Abstract

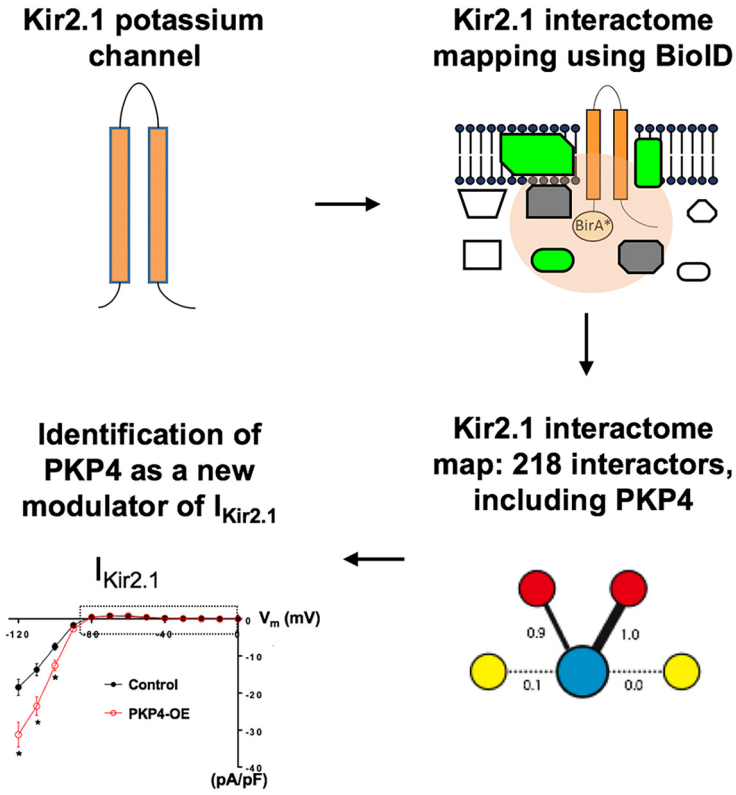


## Highlights

- Generation using BioID of a map of the Kir2.1 interactome with 218 interactions.
- Identification of Kir2.1$^{WT}$- versus Kir2.1$^{\Delta 314\text{-}315}$-preferred interactors.
- Identification of the desmosome protein PKP4 as a new modulator of $I_{Kir2.1}$ currents.


**Park et al., 2020, Mol Cell Proteomics *19(9),* 1436–1449**



**https://doi.org/10.1074/mcp.RA120.002071**

# Kir2.1 Interactome Mapping Uncovers PKP4 as a Modulator of the Kir2.1-Regulated Inward Rectifier Potassium Currents

Sung-Soo Park[1,‡], Daniela Ponce-Balbuena[2,‡], Rork Kuick[3,†], Guadalupe Guerrero-Serna[2], Justin Yoon[1], Dattatreya Mellacheruvu[1], Kevin P. Conlon[1], Venkatesha Basrur[1], Alexey I. Nesvizhskii[1,4], José Jalife[2,5,6,*], and Jean-François Rual[1,*]

**Kir2.1, a strong inward rectifier potassium channel encoded by the *KCNJ2* gene, is a key regulator of the resting membrane potential of the cardiomyocyte and plays an important role in controlling ventricular excitation and action potential duration in the human heart. Mutations in *KCNJ2* result in inheritable cardiac diseases in humans, *e.g.* the type-1 Andersen-Tawil syndrome (ATS1). Understanding the molecular mechanisms that govern the regulation of inward rectifier potassium currents by Kir2.1 in both normal and disease contexts should help uncover novel targets for therapeutic intervention in ATS1 and other Kir2.1-associated channelopathies. The information available to date on protein-protein interactions involving Kir2.1 channels remains limited. Additional efforts are necessary to provide a comprehensive map of the Kir2.1 interactome. Here we describe the generation of a comprehensive map of the Kir2.1 interactome using the proximity-labeling approach BioID. Most of the 218 high-confidence Kir2.1 channel interactions we identified are novel and encompass various molecular mechanisms of Kir2.1 function, ranging from intracellular trafficking to cross-talk with the insulin-like growth factor receptor signaling pathway, as well as lysosomal degradation. Our map also explores the variations in the interactome profiles of Kir2.1$^{WT}$ *versus* Kir2.1$^{\Delta 314\text{-}315}$, a trafficking deficient ATS1 mutant, thus uncovering molecular mechanisms whose malfunctions may underlie ATS1 disease. Finally, using patch-clamp analysis, we validate the functional relevance of PKP4, one of our top BioID interactors, to the modulation of Kir2.1-controlled inward rectifier potassium currents. Our results validate the power of our BioID approach in identifying functionally relevant Kir2.1 interactors and underline the value of our Kir2.1 interactome as a repository for numerous novel biological hypotheses on Kir2.1 and Kir2.1-associated diseases.**

The strong inward rectifier potassium channel Kir2.1 is a key regulator of the resting membrane potential of the cardiomyocyte and plays an important role in controlling ventricular excitation and action potential duration in the human heart (1–3). Both loss and gain of function mutations in *KCNJ2*, the gene encoding Kir2.1, result in inheritable cardiac ion channel diseases. For example, several *KCNJ2* loss of function mutations are associated with the inheritable type-1 Andersen-Tawil syndrome (ATS1), also known as long QT syndrome type 7, which predisposes patients to cardiac arrhythmias and sudden death (4, 5). On the other hand, *KCNJ2* gain-of function mutations give rise to the type-3 variant of the short QT syndrome, which also results in increased risk of sudden cardiac death (6). Understanding the molecular mechanisms that govern the regulation of inward rectifier potassium currents by Kir2.1 in both normal and disease contexts should help uncover novel targets for therapeutic intervention in ATS1 and other Kir2.1-associated channelopathies.

Over the last 20 years, analyses of the Kir2.1 channelosome using genetic, pharmacological, and molecular approaches have greatly contributed to our understanding of its function and its role in cardiac diseases (3, 7, 8). Expression, trafficking, localization, and function of Kir2.1 are regulated by its interactions with multiple proteins. To date, 24 putative Kir2.1 interactors have been identified, out of which 16 are high-confidence Kir2.1 interactors (supplemental Table S1). For example, Leonoudakis *et al.* showed that the PDZ-binding motif of Kir2.1 interacts with the SAP97, CASK and LIN7C proteins, members of the membrane-associated guanylate kinase (MAGUK) family, which work both as scaffolding proteins for large

From the [1]Department of Pathology, University of Michigan Medical School, Ann Arbor, MI, USA; [2]Department of Internal Medicine and Center for Arrhythmia Research, University of Michigan, Ann Arbor, MI, USA; [3]Department of Biostatistics, School of Public Health, University of Michigan, Ann Arbor, MI, USA; [4]Department of Computational Medicine & Bioinformatics, University of Michigan, Ann Arbor, MI, USA; [5]Fundación Centro Nacional de Investigaciones Cardiovasculares Carlos III, Madrid, Spain; [6]Centro de Investigación Biomédica en Red de Enfermedades Cardiovasculares, Madrid, Spain

This article contains supplemental data.

*For correspondence: Jean-François Rual, jrual@umich.edu; José Jalife, jjalife@umich.edu.

†Author deceased.

‡These authors contributed equally to this work.







DOI 10.1074/mcp.RA120.002071

macromolecular structure and as trafficking regulators (9–11). Recently, we and others demonstrated that the Kir2.1 channel and the voltage-gate sodium channel, Nav1.5, belong to common multiprotein channelosomes, enabling one to regulate the other's expression (12–15). It has become apparent that ion channel proteins do not function in isolation but are part of large, multi-protein complexes, comprising not only the ion channels and their auxiliary subunits, but also components of the cytoskeleton, regulatory post-translation modification enzymes, trafficking proteins, extracellular matrix proteins, and even other ion channels (3, 7, 8). Notwithstanding the significance of the aforementioned biochemical studies, the information available on protein-protein interactions involving Kir2.1 channels, with only 16 high-confidence Kir2.1 interactors, remains limited. Additional efforts are necessary to provide a comprehensive map of the Kir2.1 interactome.

The relatively low number of known Kir2.1 interactors described to date in the literature can be attributed to its hydrophobic nature and the technical challenges associated with its biochemical manipulation. Similarly, some members of the protein complexes associated with Kir2.1 may mediate weak, transient interactions that are lost during "standard" biochemical affinity purification in the various lysis, wash, and elution steps. BioID, a cutting-edge proximity-labeling technology that is particularly well-suited to mapping protein interactions for low-solubility proteins, overcomes many of the above barriers imposed by conventional screening methods (16–18). BioID is based on the fusion of a promiscuous *E. coli* biotin protein ligase (BirA*) to a bait protein (17). On expression of the BirA*-bait fusion protein in cell and subsequent addition of biotin, proteins that are near-neighbors of the fusion protein are biotinylated in a proximity-dependent manner. Biotinylated proteins are then isolated by affinity capture and identified by MS (MS), thus uncovering the BioID interactome of the bait protein under investigation (17). A key advantage of this proteomic approach resides in the fact that the bait, *e.g.* the low-solubility channelosome protein Kir2.1, does not need to be biochemically purified in native complex and that transient interactions can be captured (16–18).

Here, we present the generation of a comprehensive map of the Kir2.1 interactome using BioID. Bait proteins used in our BioID proteomic screens include not only Kir2.1$^{WT}$ but also Kir2.1$^{\Delta 314\text{-}315}$, an ATS1-associated mutation, which blocks Kir2.1 Golgi export (4, 19, 20). Thus, beyond interactome mapping, our BioID experiments also aim to capture the differences between the protein interaction profiles of Kir2.1$^{WT}$ *versus* Kir2.1$^{\Delta 314\text{-}315}$ proteins, and to uncover the molecular mechanisms whose malfunctions underlie ATS1 disease. A total of 218 high-confidence Kir2.1 BioID interactors were identified, including 75 Kir2.1$^{WT}$-preferred interactors, 66 Kir2.1$^{\Delta 314\text{-}315}$ mutant-preferred interactors and 77 proteins that interact with both WT and mutant Kir2.1 proteins. Finally, we present patch-clamp analyses of one of our top BioID interactors, PKP4, which validate its functional relevance to modulation of Kir2.1-regulated inward rectifier potassium currents.

## EXPERIMENTAL PROCEDURES

*Plasmids and Antibodies*—For the transmembrane protein control (TM-CTRL), the amino acid sequence IIFRTLFGSLVFAIFLILMIN of the *Saccharomyces cerevisiae* P25353 protein transmembrane domain, which has no homology to any human proteins, was selected and a humanized codon sequence was synthesized (supplemental Table S2). The protein-encoding Open Reading Frames (ORFs) of *Kir2.1*$^{WT}$ (NM_000891.2), *Kir2.1*$^{\Delta 314\text{-}315}$, and TM-CTRL were first cloned by Gateway recombination cloning from the cDNA plasmids into the Gateway Donor vector pDONR223 to generate Entry clones, as previously described (21) (primer sequences are shown in supplemental Table S2). The Gateway clone of *PKP4* (EL733946) was obtained from the Center for Cancer Systems Biology (CCSB, Harvard Medical School, Boston) human ORFeome collection (21). Protein-encoding ORF/s were then subcloned from the Entry clones into the Gateway Destination vectors pDEST-pcDNA5-FRT-BirA*-FLAG-N-term and pDEST-pcDNA3-HA (18, 22). A target sequence of *PKP4* for CRISPR/Cas9 (supplemental Table S2) was selected using CHOPCHOP web tool (23) and cloned into pX459 (Addgene, Watertown, MA, 62988), as previously described (24). The following primary and secondary antibodies were used in the Western blot analyses: FLAG (Sigma, Kawasaki, Kanagawa, Japan, A8592) and goat $\alpha$-rabbit IgG (Cell Signaling, Danvers, MA, 7074).

*Cell Culture*—Flp-In T-REx 293 cells (ThermoFisher Scientific, Waltham, MA, R78007) were maintained following the manufacturer's guideline and were transfected with the Gateway expression vectors (pcDNA5-FRT-BirA*-FLAG-N-term) of Kir2.1$^{WT}$, Kir2.1$^{\Delta 314\text{-}315}$, and TM-CTRL using polyethylenimine (Polysciences, Warrington, PA, 23966-2) (co-transfection with pOG44) as previously described (25). Stable cells were selected using 200 $\mu$g/ml hygromycin B (Invitrogen, Carlsbad, CA, 10687010). HEK293T cells were cultivated in DMEM (Invitrogen, 11995) medium supplemented with 10% FBS (Sigma, F0926) and penicillin/streptomycin (Invitrogen, 15140) and were transfected with protein expression vectors using PEI.

*Affinity Purification of Biotinylated Proteins*—BioID experiments were performed as previously described (18) with some minor modifications. Triplicate BioID experiments were performed for each of the bait proteins: BirA*-Kir2.1$^{WT}$, BirA*-Kir2.1$^{\Delta 314\text{-}315}$ and BirA*-TM-CTRL. Cells were incubated for 24 h with 10 $\mu$g/ml tetracycline and 50 $\mu$M biotin. After washing with cold PBS, cells ($n = 3 \times 10^7$) were lysed for 30 min at 4°C with lysis buffer [50 mM Tris pH 7.2, 150 mM NaCl, 10% glycerol, 1% Nonidet P-40, 0.5% sodium deoxycholate, 0.2% SDS, protease inhibitor (Roche, Basel, Switzerland, 05 056 489 001), phosphatase inhibitor (Sigma, P0044), and Benzonase (Sigma, E1014)]. The cleared cell lysates were incubated with 30 $\mu$L of streptavidin bead slurry (ThermoFisher Scientific, 20361) for 3 h at 4°C. The beads were washed with washing buffer (50 mM Tris pH 7.2, 150 mM NaCl, 10% glycerol, 1% Nonidet P-40, 0.5% sodium deoxycholate, 0.2% SDS) four times and then with rinse buffer (50 mM Tris pH 7.2, 150 mM NaCl, 0.5% Nonidet P-40) three times. The beads were washed with fresh 50 mM $NH_4HCO_3$ three times and stored at −80°C.

*Protein Identification by Mass Spectrometry and BioID Hit Selection*—The samples were analyzed in the Proteomics Resource Facility of the Department of Pathology at the University of Michigan for protein identification. Briefly, upon reduction (10 mM DTT) and alkylation (65 mM 2-chloroacetamide) of the cysteines, proteins were digested overnight with 500 ng of sequencing grade, modified trypsin (Promega, Madison, WI, V5111). Resulting peptides were resolved on a nano-capillary reverse phase column (Acclaim PepMap C18, 2 $\mu$M, 50 cm, ThermoFisher Scientific, ES803) using 0.1% formic

acid/acetonitrile (ACN) gradient at 300 nL/minute (2–25% ACN in 108 min, 25–40% in 20 min, followed by a 90% ACN wash for 10 min and a further 30 min' re-equilibration with 2% ACN) and directly introduced into Orbitrap Fusion Tribrid Mass Spectrometer (ThermoFisher Scientific). MS1 scans were acquired at 120k resolution. Data-dependent high-energy C-trap dissociation MS/MS spectra were acquired with top speed option (3 s) following each MS1 scan (relative CE ~32%). Proteins were identified by searching the data against *Homosapiens* database containing both canonical and isoform protein entries (SwissProt v2016-11-30; total number of entries: 42054) using Proteome Discoverer (v2.1, ThermoFisher Scientific, June 2016) with enzyme specificity for trypsin. Search parameters included MS1 mass tolerance of 10 ppm and fragment tolerance of 0.1 Da; two missed cleavages were allowed; carbamidomethylation of cysteine was considered fixed modification and oxidation of methionine, deamidation of asparagine and glutamine were considered as variable modifications. False discovery rate (FDR) was determined using target-decoy strategy and proteins/peptides with a FDR of $\leq$1% were retained. A stringent set of criteria were used for the selection of the high-confidence Kir2.1 BioID hits: (1) average SpC (spectral counts) in either the Kir2.1$^{WT}$ or the Kir2.1$^{\Delta 314\text{-}315}$ BioID experiment $>$ 10; (2) SAINT probability (27, 28) $>$ 0.9; and (3) primary fold change FC-A score (28) $>$ 7. The data obtained with the TM-CTRL bait were used as negative controls for the calculations. One of the high-confidence Kir2.1 BioID interactors has been identified with a single peptide, *i.e.* NACA2. The spectra annotation for NACA2 is provided in the supplemental Fig. S1.

*Kir2.1$^{WT}$ versus Kir2.1$^{\Delta 314\text{-}315}$ Interactome Profiling*—We classified the BioID hits as Kir2.1$^{WT}$-preferred or Kir2.1$^{\Delta 314\text{-}315}$ -preferred interactors based on the normalized Kir2.1$^{WT/\Delta 314\text{-}315}$ SpC ratio "*R* ". For a given protein, "*R* " represents the ratio of the SpC observed for this protein in the Kir2.1$^{WT}$ and Kir2.1$^{\Delta 314\text{-}315}$ BioID experiments. Specifically, *R* was calculated as follows. First, the number of SpC observed for a given protein in a given triplicate Kir2.1$^{WT}$ or Kir2.1$^{\Delta 314\text{-}315}$ BioID experiment was normalized to the Kir2.1$^{WT}$ BioID experiment #1 by dividing SpC by the ratio of the Kir2.1 SpC observed in this given experiment to the Kir2.1 SpC observed in the Kir2.1$^{WT}$ BioID experiment #1 (supplemental Table S3, columns X-AE). Second, after adding one to each SpC and $Log_2$-transformation (columns AF-AK), we calculated the average $Log_2$-transformed, normalized SpC for both the Kir2.1$^{WT}$ and Kir2.1$^{\Delta 314\text{-}315}$ BioID experiments (columns AL and AM). The ratio *R* was then calculated by performing a power of 2 transformation (column AN). The statistical significances of the difference between the Kir2.1$^{WT}$ and Kir2.1$^{\Delta 314\text{-}315}$ BioID experiments were computed using a two-sample *t* test on the $Log_2$-transformed data (column AO). Kir2.1 BioID hits with both $R > 2$ and $p < 0.05$ were classified as Kir2.1$^{WT}$-preferred interactors whereas proteins with both $R < 0.5$ and $p < 0.05$, *i.e.* a 2-fold decrease, were classified as Kir2.1$^{\Delta 314\text{-}315}$-mutant preferred interactors (column AP). A permutation analysis was performed to estimate the false discovery rate ($FDR < 0.007$).

*Immunofluorescence (IF) Staining Experiments*—IF staining experiments were performed utilizing either HEK293 cells or freshly isolated rat ventricular myocytes, as previously described (15) using the following primary and secondary antibodies: PKP4 (ThermoFisher Scientific, PA5-66855, dilution 1/500), Kir2.1 (Alomone Labs, Jerusalem, Israel, AGP-044, dilution 1/20), Actinin (Sigma, SAB4503474, 1/300), GM130 (Novus Biologicals, NBP2-53420; dilution 1/200), FLAG (Sigma-Aldrich; F3165, dilution: 1/50), Alexa Fluor 488 donkey anti-mouse, Alexa Fluor 594 donkey anti-guinea pig and Alexa Fluor 647 donkey anti-rabbit (Jackson ImmunoResearch, West Grove, PA, dilution 1/400).

*Patch-Clamping Experiments*—HEK293 cells were grown in 60-mm dishes and, upon reaching ~60–70% confluence, were transiently transfected using X-tremeGENE HP DNA transfection reagent (Sigma, 6366244001) following the supplier's directions. The DNA plasmids used in the patch-clamp experiments were: CRISPR/Cas9 construct pX459-gPKP4 and negative control pX459 and protein expression vectors pcDNA3-HA-PKP4 and "empty vector" negative control pcDNA3-HA. A GFP-expression vector was also co-transfected to visualize the transfected cells during the patch-clamp experiments. Patch-clamp experiments were performed 48 h after transfection, as previously described (12, 13, 15). Inward rectifier potassium currents ($I_{Kir2.1}$) were recorded at room temperature (21–23 °C) using the whole-cell patch-clamp technique and filtered at half the sampling frequency (12, 13, 15). Series resistance was compensated manually and $\geq$80% compensation was achieved. Under our experimental conditions, no significant voltage errors (<5 mV) because of series resistance were expected with the micropipettes used.

*Experimental Design and Statistical Rationale*—The total number of samples analyzed and the statistical tests used in the various experiments are indicated throughout the text, *e.g.* triplicate BioID experiments were performed, the number of transfected cell batches (*N*) and number of cells (*n*) used in the patch-clamping experiments are shown, or the statistical significances of the difference between the Kir2.1$^{WT}$ and Kir2.1$^{\Delta 314\text{-}315}$ BioID experiments were computed using a two-sample *t* test on the $Log_2$-transformed data.

## RESULTS AND DISCUSSION

*Kir2.1 Interactome Mapping Using BioID*—Using the proximity-labeling technology BioID (16–18), we generated a map of the Kir2.1 interactome (overall procedure is described in Fig. 1). Both Kir2.1$^{WT}$ and Kir2.1$^{\Delta 314\text{-}315}$, an ATS-associated mutant protein for which Golgi export is impaired (4, 19, 20), were used as BirA*-tagged BioID baits. We performed patch-clamping analyses of both the BirA*-tagged Kir2.1$^{WT}$ and Kir2.1$^{\Delta 314\text{-}315}$ bait proteins (supplemental Fig. S2). As expected, HEK293 cells expressing BirA*-tagged Kir2.1$^{WT}$, but not mutant BirA*-tagged Kir2.1$^{\Delta 314\text{-}315}$ cells, exhibited the characteristic ability to strongly rectify, that is to pass $K^+$ current in the inward direction much more readily than outward. Moreover, BirA*-tagged Kir2.1$^{WT}$ channels maintain their sensitivity to $Ba^{2+}$ blocking (supplemental Fig. S2). As a negative control, we used the TM-CTRL construct, a yeast transmembrane domain fused to the BioID BirA* tag. We investigated the subcellular localization of both Kir2.1$^{WT}$ and Kir2.1$^{\Delta 314\text{-}315}$ bait proteins as well as the TM-CTRL by IF staining (supplemental Fig. S3). After expression of the BirA*-Kir2.1$^{WT}$, BirA*-Kir2.1$^{\Delta 314\text{-}315}$ and BirA*-TM-CTRL bait proteins in HEK293 cells (supplemental Fig. S4) and purification of the biotinylated proteins on streptavidin-agarose beads, the purified protein extracts were subjected to MS/MS analysis for identification. The Kir2.1$^{WT}$, Kir2.1$^{\Delta 314\text{-}315}$ and TM-CTRL baits were each assessed in triplicate BioID experiments. A stringent set of criteria were used for the selection of the Kir2.1 BioID hits: i) average SpC in either the Kir2.1$^{WT}$ or the Kir2.1$^{\Delta 314\text{-}315}$ BioID experiments $>$ 10; ii) SAINT probability score (27, 28) $>$ 0.9; and iii) primary fold change FC-A score (28) $>$7. Our proteomic screen resulted in the identification of 218 high-confidence

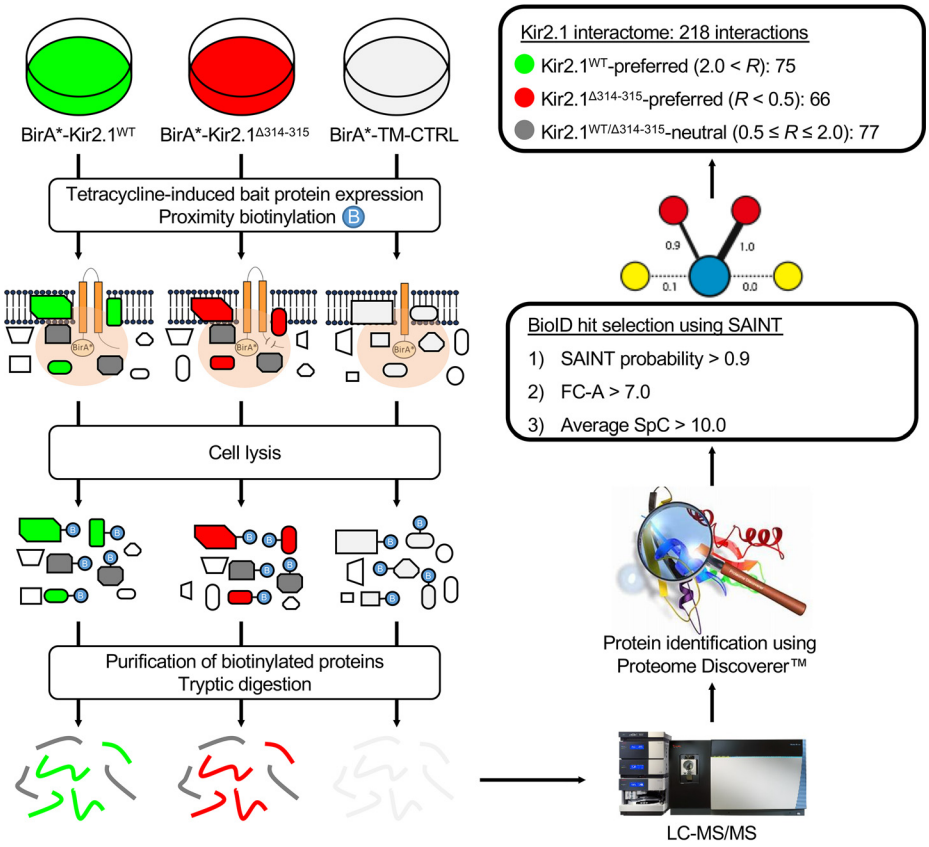


FIG. 1. **Overall procedure to generate the Kir2.1 BioID interactome map.** Stable cells expressing BirA*-tagged Kir2.1$^{WT}$, Kir2.1$^{\Delta 314-315}$ or TM-CTRL bait proteins were generated using the Flp-In T-Rex 293 cell line. Expression of the bait proteins was induced by tetracycline and cells were treated with Supplemental biotin for 24 h. After cell lysis, biotinylated proteins were purified on streptavidin-agarose beads and digested with trypsin. Tryptic peptides were analyzed using LC–MS/MS and proteins were identified using Proteome Discoverer. After applying a stringent set of criteria, we identified 218 high-confidence Kir2.1 BioID hits. Using the normalized Kir2.1$^{WT/\Delta 314-315}$ SpC ratio "*R* ", we classified the interactors in three categories: 75 Kir2.1$^{WT}$-preferred interactors, 66 Kir2.1$^{\Delta 314-315}$-preferred interactors and 77 Kir2.1$^{WT/\Delta 314-315}$-neutral interactors. CTRL: control; LC–MS/MS: liquid chromatography with tandem MS; SAINT: Significance Analysis of INTeractome; SpC: spectral counts; TM: transmembrane; WT: WT.

Kir2.1 BioID hits, the vast majority of which are novel putative Kir2.1 direct or indirect interactors (supplemental Table S3). Interestingly, some of the newly identified BioID interactors include products of genes previously associated with physiological or pathophysiological function of the myocardium, *e.g.* UTRN (29, 30) and PKP4 (31, 32), as described in detail below. Curation of the literature and of the functional data reported in PubMed for each of these genes led to the identification of a dozen of known protein complexes or functionally related biological modules in our list of 218 high-confidence Kir2.1 BioID hits, *e.g.* the cadherin adhesome and the COPII complex.

To assess the sensitivity of our BioID proteomic screen, we measured the proportion of the previously described Kir2.1 interactors that are also present in our list of 218 high-confidence Kir2.1 BioID interactors. A review of several protein interaction repositories [BioGRID (33), IntAct (34), HPRD (35), HuRI (36, 37)] identified 24 putative Kir2.1 protein interactions. After literature curation, we selected 16 high-confidence Kir2.1 interactions that had been observed in at least two experiments and/or validated for their functional relevance (supplemental Table S1). We note, though, that some of these interactions have been studied using the *Mus musculus* or *Rattus norvegicus* proteins, but not the human proteins (columns I–J in supplemental Table S1). Out of all the 24 previously reported putative Kir2.1 interactors, 10 (~42%) were identified in our BioID screen. Similarly, out of the 16 high-confidence Kir2.1 interactions, 7 (~44%) were identified in our BioID screen, *i.e.* SAP97, CASK, CAV1, LIN7C, AKAP5, Kir2.6 and Kir2.3 (supplemental Table S1 and S3). This analysis suggests a high sensitivity of >40% for our BioID assay. By comparison, the sensitivity of high-throughput protein interaction mapping assays used on a proteome-scale ranges from ~20 to ~35% (38).

*Kir2.1$^{WT}$ versus Kir2.1$^{\Delta 314-315}$ Interactome Profiling*—Understanding the molecular mechanisms that govern the regulation of inward rectifier potassium currents by Kir2.1 in both normal and disease contexts should help uncover novel

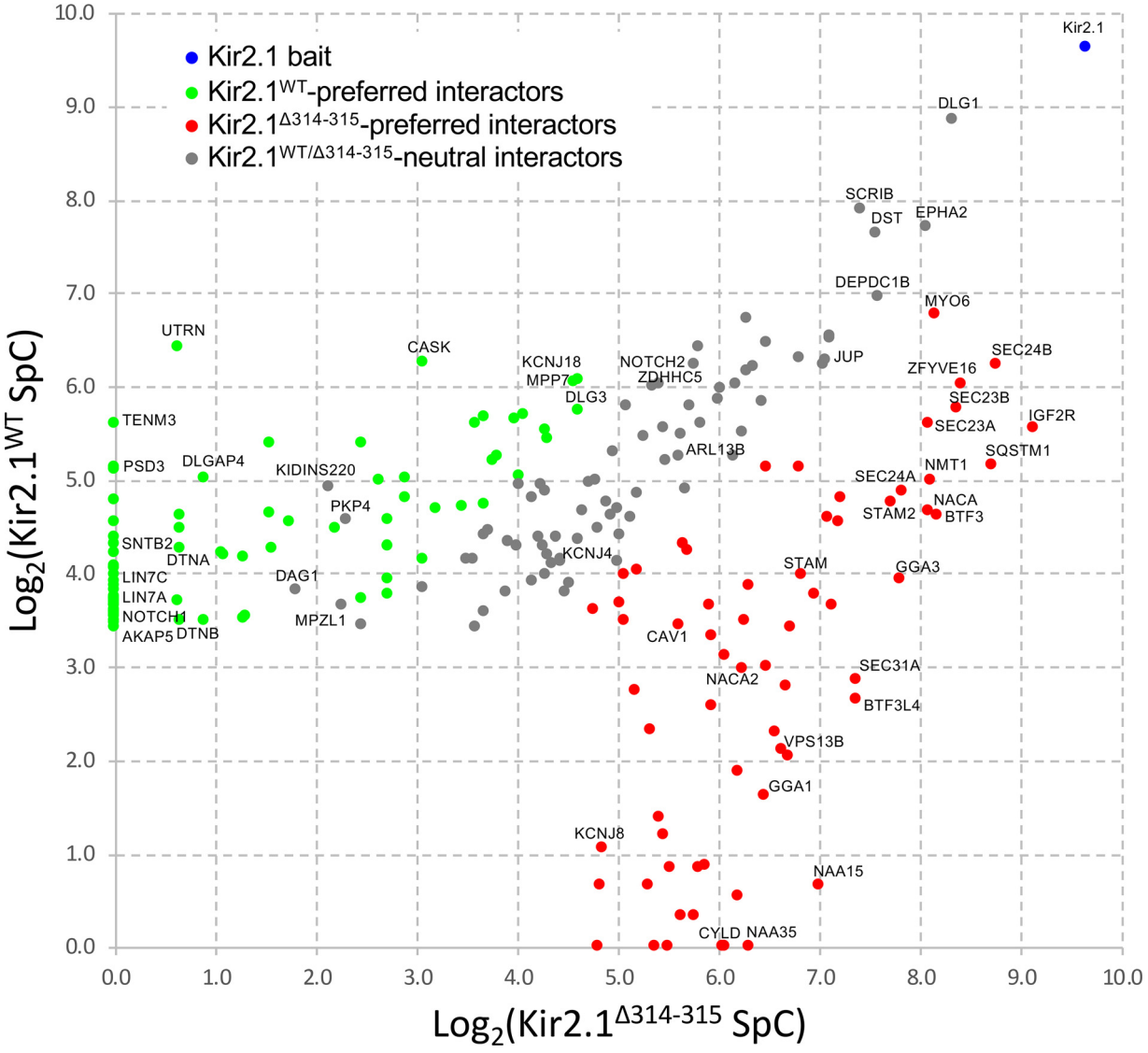


FIG. 2. **Kir2.1$^{WT}$ *versus* Kir2.1$^{\Delta 314-315}$ interactome profiling.** Variations in the Kir2.1$^{WT}$ and Kir2.1$^{\Delta 314-315}$ interactome profiles are visualized in a scatter plot representing the average $Log_2$-transformed, normalized SpC counts for both the Kir2.1$^{WT}$ (*y* axis) and Kir2.1$^{\Delta 314-315}$ (*x* axis) bait proteins. The Kir2.1 bait, Kir2.1$^{WT}$-preferred interactors, Kir2.1$^{\Delta 314-315}$-preferred interactors and Kir2.1$^{WT/\Delta 314-315}$-neutral interactors are represented as blue, green, red and gray dots, respectively.

targets for therapeutic intervention in ATS1 and other Kir2.1-associated channelopathies. Beyond interaction mapping, our proteomic experiments also aims at capturing the differences between the interaction profiles of Kir2.1$^{WT}$ and Kir2.1$^{\Delta 314-315}$. Using the normalized Kir2.1$^{WT/\Delta 314-315}$ SpC ratio "*R*" (supplemental Table S3, columns AN-AP; see Methods for details about the calculation, normalization and statistical analysis), we classified the 218 high-confidence Kir2.1 BioID hits: 75 tend to interact preferentially with Kir2.1$^{WT}$, 66 interact preferentially with Kir2.1$^{\Delta 314-315}$ and the remaining 77 BioID interactors interact with both the Kir2.1$^{WT}$ and Kir2.1$^{\Delta 314-315}$ proteins (*FDR* $<$ 0.007; Fig. 2). For example, the normalized SpC counts for UTRN in the BioID experiments are: 86.0 SpC for Kir2.1$^{WT}$ and 0.9 SpC for Kir2.1$^{\Delta 314-315}$, *i.e.* $r = 56.0$ and $p = 8 \times 10^{-4}$. UTRN is thus classified as a Kir2.1$^{WT}$-preferred interactor.

The ATS1-associated mutation Kir2.1$^{\Delta 314-315}$ blocks Kir2.1 Golgi export (4, 19, 20). Hence, Kir2.1$^{WT}$-preferred interactors may encompass both: i) protein interactors that are directly involved in the normal trafficking of Kir2.1, and ii) protein interactors that, as an indirect consequence of the Golgi-trapping, do not interact with Kir2.1$^{\Delta 314-315}$ simply because it is not present at the plasma membrane. Interestingly, out of the 75 Kir2.1$^{WT}$-preferred interactors, 13 of them have been associated (mutation and/or GWAS hit) with one or several heart-related traits or diseases, *e.g.* atrial fibrillation (AF) or systolic/diastolic blood pressure (supplemental Table S3, column AR).

Most ATS mutants, including Kir2.1$^{\Delta 314\text{-}315}$, exert a dominant-negative effect on Kir2.1$^{WT}$ channels, as oppose to an haploinsufficiency effect (20). Accordingly, protein interactions involving Kir2.1$^{\Delta 314\text{-}315}$-preferred interactors may also encompass molecular mechanisms that are not properly regulated in the presence of Kir2.1$^{\Delta 314\text{-}315}$. For example, the Kir2.1$^{\Delta 314\text{-}315}$ mutation may result in the gain of an interaction (or increased binding affinity) between Kir2.1$^{\Delta 314\text{-}315}$ and a protein present in the Golgi that perturbs normal trafficking and results in the trapping of Kir2.1$^{\Delta 314\text{-}315}$. On one hand, the increased ability for Kir2.1$^{\Delta 314\text{-}315}$ to interact with some of these Kir2.1$^{\Delta 314\text{-}315}$-mutant preferred interactors may be an indirect consequence of the Δ314-315 mutation and these Kir2.1$^{\Delta 314\text{-}315}$-mutant preferred interactors are thus likely to have low relevance to the disease. On the other hand, the increased ability for Kir2.1$^{\Delta 314\text{-}315}$ to interact with some of these Kir2.1$^{\Delta 314\text{-}315}$-mutant preferred interactors may be a direct consequence of the Δ314-315 mutation and some of these Kir2.1$^{\Delta 314\text{-}315}$-mutant preferred interactors may thus be possible direct contributing factors to the disease. Interestingly, out of the 66 Kir2.1$^{\Delta 314\text{-}315}$-preferred interactors, 10 of them have been associated (mutation and/or GWAS hit) with one or several heart-related traits or diseases, *e.g.* atrial fibrillation (AF) or systolic/diastolic blood pressure (supplemental Table S3, column AR). Below, we discuss in details the potential implications associated with some of these Kir2.1$^{WT}$-preferred interactors, *e.g.* UTRN, and Kir2.1$^{\Delta 314\text{-}315}$-preferred interactors, *e.g.* NAC and IGF1R.

The analysis of the variations in the interactome profiles of Kir2.1$^{WT}$ and Kir2.1$^{\Delta 314\text{-}315}$ allows us to identify protein complexes or groups of functionally related proteins that, for the most part, tend to interact primarily with either Kir2.1$^{WT}$ or Kir2.1$^{\Delta 314\text{-}315}$ (Fig. 3). For example, most of the proteins in the MAGUK complex interact preferentially with Kir2.1$^{WT}$ (colored in green in Fig. 3). In contrast, Kir2.1 interactors in the Nascent polypeptide-associated complex (NAC) bind preferentially to Kir2.1$^{\Delta 314\text{-}315}$ (colored in red in Fig. 3). Interestingly, the "Channels-Transporters" group encompasses proteins that interact preferentially with either cytoplasmic membrane-bound Kir2.1$^{WT}$, Golgi-trapped Kir2.1$^{\Delta 314\text{-}315}$ or that are Kir2.1$^{WT/\Delta 314\text{-}315}$-neutral interactors (colored in gray in Fig. 3). This observation indicates that Kir2.1 not only interacts with other channels-transporters at the cytoplasmic membrane but that the co-trafficking of these proteins in the endoplasmic reticulum (ER) and Golgi apparatus is an important aspect of their function. Thus, the previously described dynamic reciprocity for the regulation of $Na_v1.5$ sodium and Kir2.1 potassium channel expression, which controls cardiac excitability and arrhythmia (12), likely extends to other channelosome protein complexes beyond $Na_v1.5$.

*Enrichment Analyses*—To further extend our analysis of the protein complexes and the groups of genes that interact with Kir2.1, we performed a gene set enrichment analysis using DAVID (39) (supplemental Table S4). We observed that Kir2.1$^{WT}$-preferred interactors are enriched for protein families involved in cell adhesion [GO:0007155, Fold Enrichment (FE) = 8, $p = 2 \times 10^{-8}$], including integrin complex proteins (GO:0008305, FE = 55, $p = 6 \times 10^{-8}$) and cadherin adhesome proteins (GO:0098641, FE = 6.1, $p = 9 \times 10^{-4}$). In addition to the protein domains characteristic of integrin proteins, *e.g.* InterPro domain IPR018184 (FE = 94, $p = 3 \times 10^{-9}$), Kir2.1$^{WT}$-preferred interactors also tend to contain PDZ domains (IPR001478, FE = 15, $p = 2 \times 10^{-7}$), further highlighting the previously described key role of PDZ domain-scaffolding proteins in the modulation of Kir2.1 channelosomes (8). As expected, top KEGG pathways enriched in Kir2.1$^{WT}$-preferred interactors include arrhythmogenic right ventricular cardiomyopathy (hsa05412), dilated cardiomyopathy (hsa05414) and hypertrophic cardiomyopathy (hsa05410) ($FE > 17$, $p < 2 \times 10^{-5}$).

In contrast, Kir2.1$^{\Delta 314\text{-}315}$-preferred interactors are enriched for protein families involved in many aspects of intracellular protein transport (GO:0006886, FE = 16, $p = 3 \times 10^{-12}$), including COPII (GO:0030127, FE = 145, $p = 3 \times 10^{-8}$) and ER to Golgi transport (GO:0012507, FE = 22, $p = 7 \times 10^{-4}$). On the same note, seven proteins containing the multipurpose docking adapter VHS domain, *e.g.* TOM1 and STAM, which are associated with vesicular trafficking, are enriched among the Kir2.1$^{\Delta 314\text{-}315}$-preferred interactors (IPR002014, FE = 222, $p = 1 \times 10^{-13}$). Thus, in agreement with the previous reports (4, 19, 20), our data show that ATS1 pathogenesis associated with the Kir2.1$^{\Delta 314\text{-}315}$ mutation underlies malfunctions in the mechanisms governing Kir2.1 trafficking from the Golgi to the cytoplasmic membrane.

Kir2.1$^{\Delta 314\text{-}315}$-preferred interactors are also linked to ESCRT-0 (GO:0033565, FE = 289, $p = 3 \times 10^{-5}$) and lysosome (hsa04142, FE = 7, $p = 0.02$), suggesting that this ATS1 mutation leads to increased targeting of Kir2.1 to lysosomal degradation. These observations agree with the previous report by Kolb *et al.* that Kir2.1 degradation is primarily lysosomal dependent and requires ESCRT (40). However, using a pharmacological approach to inhibit either proteasomal or vacuolar proteases, Kolb *et al.* also observed that Kir2.1$^{\Delta 314\text{-}315}$ mutation targets the channel for proteasomal degradation rather than vacuolar-dependent degradation (40). Though we indeed note the presence of PSMD1, the 26S proteasome nonATPase regulatory subunit 1, among the Kir2.1$^{\Delta 314\text{-}315}$-preferred interactors, our enrichment analysis does not provide support to the "proteasome hypothesis" but instead, strongly suggests that vacuolar-dependent degradation remains an important route responsible for the increased Kir2.1$^{\Delta 314\text{-}315}$ protein turnover.

Strikingly, all the aforementioned functional attributes and the vast majority of the gene sets are specifically enriched in either Kir2.1$^{WT}$-preferred interactors or Kir2.1$^{\Delta 314\text{-}315}$-preferred interactors, but not both. For example, out of the top 30 gene sets enriched for Kir2.1$^{WT}$-preferred interactors ($p < 1 \times 10^{-3}$), only one was also enriched in the Kir2.1$^{\Delta 314\text{-}315}$-preferred

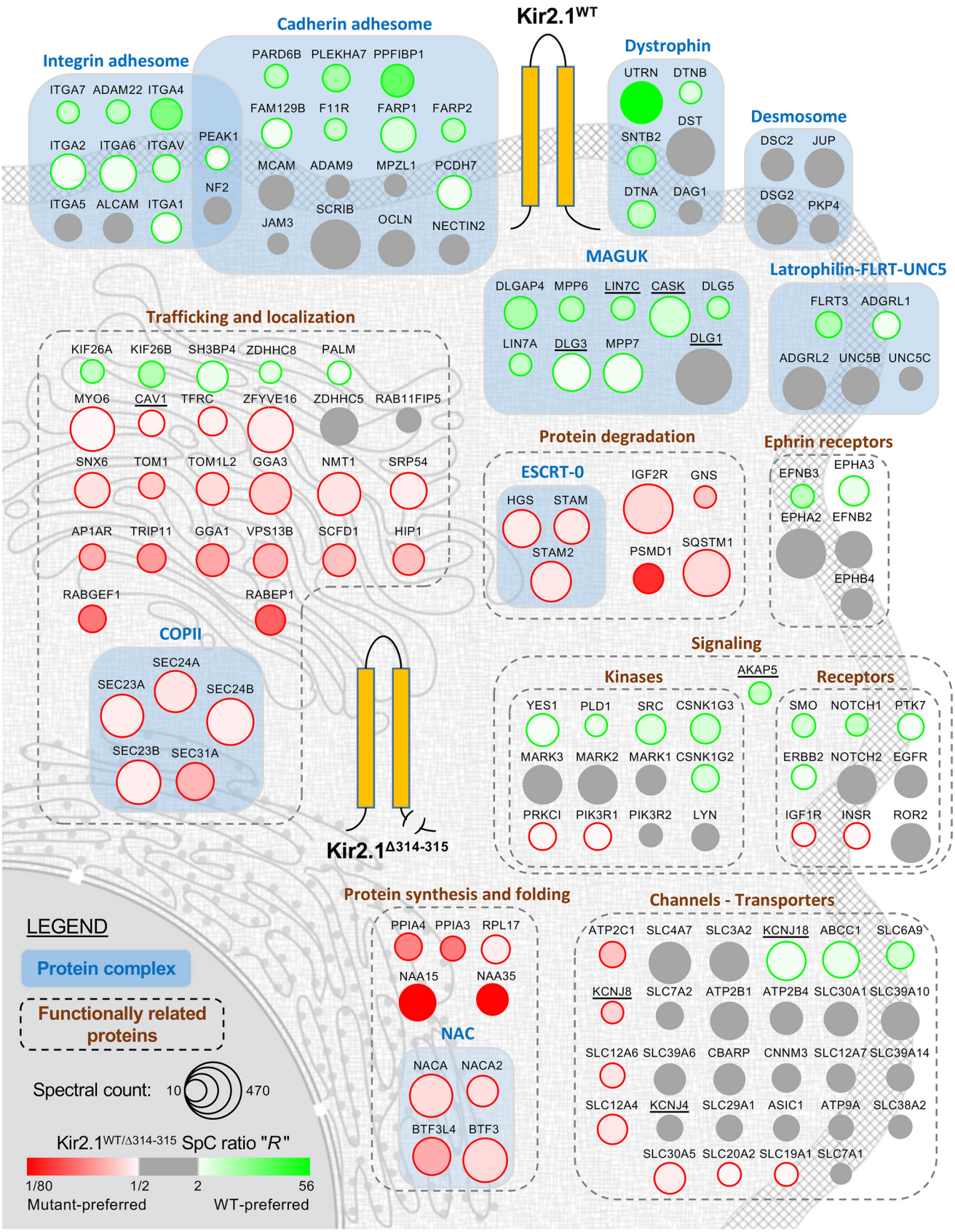
Kir2.1WT
Cadherin adhesome
PARD6B PLEKHA7 PPFIBP1
FAM129B F11R FARP1 FARP2
MCAM ADAM9 MPZL1 PCDH7
JAM3 SCRIB OCLN NECTIN2
Integrin adhesome
ITGA7 ADAM22 ITGA4
ITGA2 ITGA6 ITGAV
ITGA5 ALCAM ITGA1
PEAK1
NF2
Dystrophin
UTRN DTNB
DST
SNTB2
DTNA DAG1
Desmosome
DSC2 JUP
DSG2 PKP4
MAGUK
DLGAP4 MPP6 LIN7C CASK DLG5
LIN7A DLG3 MPP7 DLG1
Latrophilin-FLRT-UNC5
FLRT3 ADGRL1
ADGRL2 UNC5B UNC5C
Trafficking and localization
KIF26A KIF26B SH3BP4 ZDHHC8 PALM
MYO6 CAV1 TFRC ZFYVE16 ZDHHC5 RAB11FIP5
SNX6 TOM1 TOM1L2 GGA3 NMT1 SRP54
AP1AR TRIP11 GGA1 VPS13B SCFD1 HIP1
RABGEF1 RABEP1
COPII
SEC24A
SEC23A SEC24B
SEC23B SEC31A
Protein degradation
ESCRT-0
HGS STAM
STAM2
IGF2R GNS
PSMD1 SQSTM1
Ephrin receptors
EFNB3 EPHA3
EPHA2 EFNB2
EPHB4
Kir2.1Δ314-315
Signaling
Kinases
YES1 PLD1 SRC CSNK1G3
MARK3 MARK2 MARK1 CSNK1G2
PRKCI PIK3R1 PIK3R2 LYN
AKAP5
Receptors
SMO NOTCH1 PTK7
ERBB2 NOTCH2 EGFR
IGF1R INSR ROR2
Protein synthesis and folding
PPIA4 PPIA3 RPL17
NAA15 NAA35
NAC
NACA NACA2
BTF3L4 BTF3
Channels - Transporters
ATP2C1 SLC4A7 SLC3A2 KCNJ18 ABCC1 SLC6A9
KCNJ8 SLC7A2 ATP2B1 ATP2B4 SLC30A1 SLC39A10
SLC12A6 SLC39A6 CBARP CNNM3 SLC12A7 SLC39A14
SLC12A4 KCNJ4 SLC29A1 ASIC1 ATP9A SLC38A2
SLC30A5 SLC20A2 SLC19A1 SLC7A1
LEGEND
Protein complex
Functionally related proteins
Spectral count: 10 470
Kir2.1WT/Δ314-315 SpC ratio "R"
1/80 1/2 2 56
Mutant-preferred WT-preferred

interactors: basolateral plasma membrane (GO:0033565, FE = 6, $p$ = 0.02) (supplemental Table S5). Similarly, out of the top 34 gene sets enriched for Kir2.1$^{\Delta 314\text{-}315}$-preferred interactors ($p < 1 \times 10^{-3}$), only two were also enriched in the Kir2.1$^{WT}$-preferred interactors (supplemental Table S5). This observation further underscores the fact that the Kir2.1$^{WT}$ and Kir2.1$^{\Delta 314\text{-}315}$ proteins obey to dramatically different fates in the cell.

*Kir2.1 BioID Interactome: A Repository for Novel Biological Hypotheses*—The Kir2.1 BioID interactome data set represents a repository for numerous, novel biological hypotheses for genes and molecular mechanisms implicated in Kir2.1-associated cardiomyopathies. For example, out of the 218 high-confidence Kir2.1 interactors identified in our BioID screen, 37 of them have been associated (mutation and/or GWAS hit) with one or several heart-related traits or diseases, *e.g.* atrial fibrillation (AF) or systolic/diastolic blood pressure (supplemental Table S3, column AR). Below, we describe a few examples: UTRN, NACA, IGF1R and PKP4.

*UTRN* was identified in our BioID screen as a Kir2.1$^{WT}$-preferred interactor (normalized SpC counts: Kir2.1$^{WT}$: 86.0 and Kir2.1$^{\Delta 314\text{-}315}$: 0.9; supplemental Table S3). *Utrophin* deficiency worsens cardiac contractile dysfunction present in *dystrophin*-deficient mice (29). Interestingly, a race-stratified genome-wide gene-environment interaction association study recently identified polymorphic variations in the *UTRN* gene locus as potential risk factors in peripheral arterial disease (30). UTRN is part of the Dystrophin-associated proteins (DAP) complex (41) and several other DAP proteins interact with and modulate both sodium and potassium channelosome protein complexes (8, 11, 42). This novel Kir2.1-UTRN interaction further underlines the role of DAP in regulating these complexes and malfunction of these molecular mechanisms may contribute to pathophysiological conditions of the myocardium.

*Nascent-Polypeptide-Associated Complex (NAC)*—Our BioID screen identified four NAC-associated proteins as Kir2.1$^{\Delta 314\text{-}315}$-preferred interactors, *i.e.* NACA, NACA2, BTF3 and BTF3L4. For example, the normalized SpC counts for NACA are as follows: Kir2.1$^{WT}$: 24.4 and Kir2.1$^{\Delta 314\text{-}315}$: 270.7 (supplemental Table S3). The heterodimeric NAC protein complex binds to newly synthesized polypeptide chains that lack a signal peptide motif as they emerge from the ribosome, blocking interaction with the signal recognition particle (SRP) and preventing mistranslocation to the endoplasmic reticulum (43). Potential roles for NAC complex thus range from protein folding chaperone to negative regulator of translocation into the endoplasmic reticulum (43). We note, though, that NACA has also been described as a transcription factor (44), *e.g.* in collaboration with the heart-specific HDAC-dependent repressor SMYD1 (45). The roles of NACA and NAC in the cell remain to be comprehensively characterized.

Several observations link NACA to heart biology and diseases. For example, GWAS studies have identified *NACA* gene variants as potential risk factors in atrial fibrillation (AF) (46, 47), or as a regulator of myocardial mass (48). In both *Drosophila melanogaster* flies and *Danio rerio* zebrafish, the knock-down of *NACA*, *i.e.* fly *NAC*$\alpha$ and zebrafish *skNAC,* results in severe cardiac muscle defects (48, 49). In mouse, *Naca* deficiency results in embryonic lethality with cardiac developmental defects (50). Park *et al.* originally linked this phenotype to the role of NACA as a transcription factor and as a major binding partner for SMYD1 in the developing heart (50). The Kir2.1-NACA interaction suggests a more complex role for NACA in the myocardium. Indeed, Kir2.1 deficiency results not only in the loss of inward rectifier potassium currents but also in developmental defects and dysmorphic features, *e.g.* low-set ears, wide-set eyes, small mandible, clinodactyly and syndactyly (4, 5, 51–53). The molecular mechanism underlying these dysmorphic features is poorly understood. The Kir2.1-NACA interaction provides a biophysical bridge between the respective roles of these two proteins during biological development in general and cardiomyogenesis in particular.

*Cross-talks between Kir2.1 and Signal Transduction Pathways*—The Kir2.1 interactor data set as a whole is enriched for proteins involved in various aspects of signal transduction, *i.e.* enrichment is observed for all three classes of Kir2.1 interactors (WT, mutant and neutral; GO:0007165, FE > 2.4, $p < 0.01$). Each class of interactors is enriched with different signaling pathways, though. Examples of signaling pathways over-represented in our Kir2.1$^{WT}$-preferred interactor data set include the ephrin receptor signaling pathway (GO:0048013, FE = 12, $p = 5 \times 10^{-3}$) and the Hedgehog signaling pathway (KEGG hsa04340, FE = 26, $p = 5 \times 10^{-3}$).

Likewise, the Kir2.1$^{\Delta 314\text{-}315}$-preferred interactors are enriched for proteins involved in the insulin-like growth factor receptor signaling pathway, *e.g.* IGF1R and INSR (GO:0048009, FE = 57, $p = 1 \times 10^{-3}$). The normalized SpC counts for IGF1R and INSR are as follows: Kir2.1$^{WT}$: 12.1 and 15.7, and for Kir2.1$^{\Delta 314\text{-}315}$: 31.6 and 35.4, respectively (supplemental Table S3). GWAS studies have identified *IGF1R* gene variants as potential risk factors in atrial fibrillation (AF) (46, 47), as well as a regulator of myocardial mass

FIG. 3. **Graphical representation of the Kir2.1 BioID interactome.** Protein complexes and groups of functionally related proteins encompassing 152 out of the 218 high-confidence Kir2.1 BioID hits are depicted in a cell. Major organelles in the cell (nucleus, endoplasmic reticulum, Golgi apparatus and cytoplasmic membrane) are shown (light gray) in the background to roughly indicate the approximate subcellular localization of the proteins in the cell. The Kir2.1$^{WT}$-preferred interactors, Kir2.1$^{\Delta 314\text{-}315}$-preferred interactors and Kir2.1$^{WT/\Delta 314\text{-}315}$-neutral interactors are represented as green, red and gray circles, respectively. The color intensity of each circle is an indicator of the strength of the normalized Kir2.1$^{WT/\Delta 314\text{-}315}$ SpC ratio "*R*" value. The size of each circle represents the average SpC counts observed in either the Kir2.1$^{WT}$ or Kir2.1$^{\Delta 314\text{-}315}$ BioID experiment (whichever is the largest is represented in the figure).

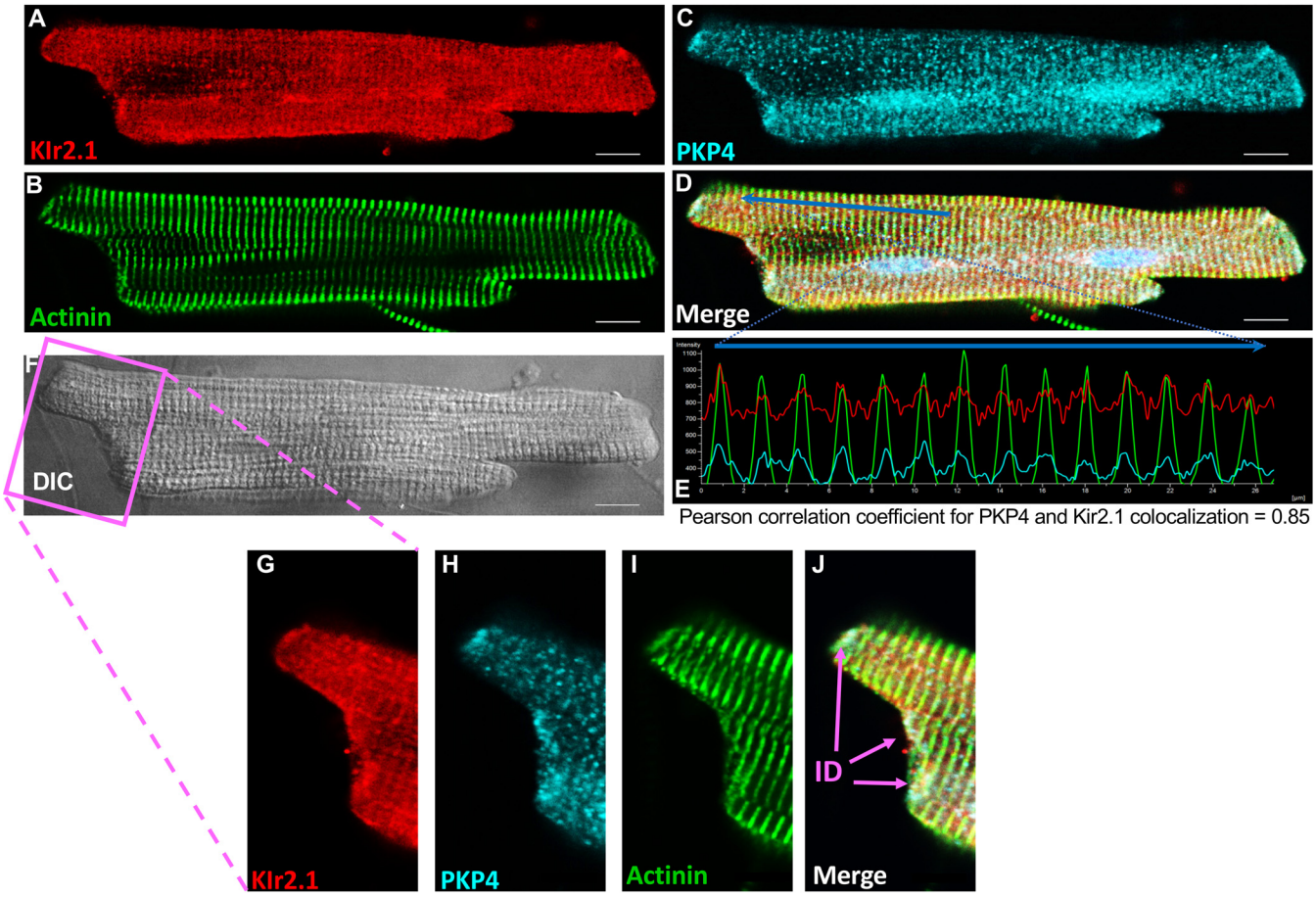


FIG. 4. **Kir2.1 and PKP4 co-localize in adult ventricular myocytes.** Immunofluorescence (IF) staining analyses of the subcellular localization of Kir2.1 (*A*, *red*), Actinin (*B*, *green*) and PKP4 (*C*, light *blue*) in a freshly isolated rat adult ventricular myocytes. (*D*) Merge image. (*E*) Pixel intensity profile of PKP4, Kir2.1 and actinin along a line in the merge image, *i.e.* blue arrow shown in (*D*) showing the striated co-localization of the three proteins at the z-disks near the cardiac sarcomeres. (*F*) Differential interference contrast (DIC) image of the myocyte. (*G–J*) Zoomed in images of the intercalated disks. Scale bars: 10 $\mu$M. ID: intercalated disk.

(48) and global electrical heterogeneity ECG (54). We hypothesize that the Kir2.1-IGF1R interaction is part of a molecular mechanism that underlies the functional associations between IGF1R and cardiac physiology.

Could the Kir2.1-IGF1R interaction also help better understand the potential role of Kir2.1 in diabetes? A functional link between Kir2.1 and the insulin-like growth factor receptor signaling pathway has been previously proposed. As early as 1998, Wischmeyer *et al.* observed that treatment of *Xenopus* oocytes with insulin was found to robustly suppress $I_{Kir2.1}$ (55). Electrical activity plays a central role in glucose-stimulated insulin secretion from human pancreatic $\beta$-cells. We note that Kir2.1 is expressed in human pancreatic islets (56) and that functional Kir2.1 currents are present in human $\beta$-cells (57). Riz *et al.* predicted that blocking Kir2.1 channels increases the rate of insulin secretion and that hyperactive Kir2.1 channels may lead to reduced insulin secretion (57). Similarly, in a recent mathematical model, Kir2.1 was predicted to be a critical actor in the regulation of oscillations in cellular activity that underlie insulin pulsatility in pancreatic islets cells lacking K(ATP) channels (58). On the same note, several publications link abnormal QT interval regulation and diabetes (59–61). Moreover, patients with long QT syndrome associated to potassium channel deficiency, *e.g.* KCNQ1 mutants, suffer from over-secretion of insulin, hyperinsulinemia, and symptomatic hypoglycemia (62). Our BioID data suggest that these functional associations between Kir2.1 and the insulin pathway need not be indirect but may also be mediated by biophysical interactions between Kir2.1 channels and insulin pathway proteins.

*Desmosome*—Several desmosome-associated proteins interact with both $Kir2.1^{WT}$ and $Kir2.1^{\Delta 314\text{-}315}$, *e.g.* JUP, DSG2, DSC2 and PKP4 (supplemental Table S3). Desmosomes act as mechanical cell-cell adhesion junctions maintaining the structural integrity of the tissue. Mutations in the *JUP*, *DSG2* and *DSC2* genes have been associated with Arrhythmogenic Right Ventricular Cardiomyopathy (ARVC) (63). Actually, with ~half of ARVC patients carrying a mutation in one of the genes encoding desmosomal

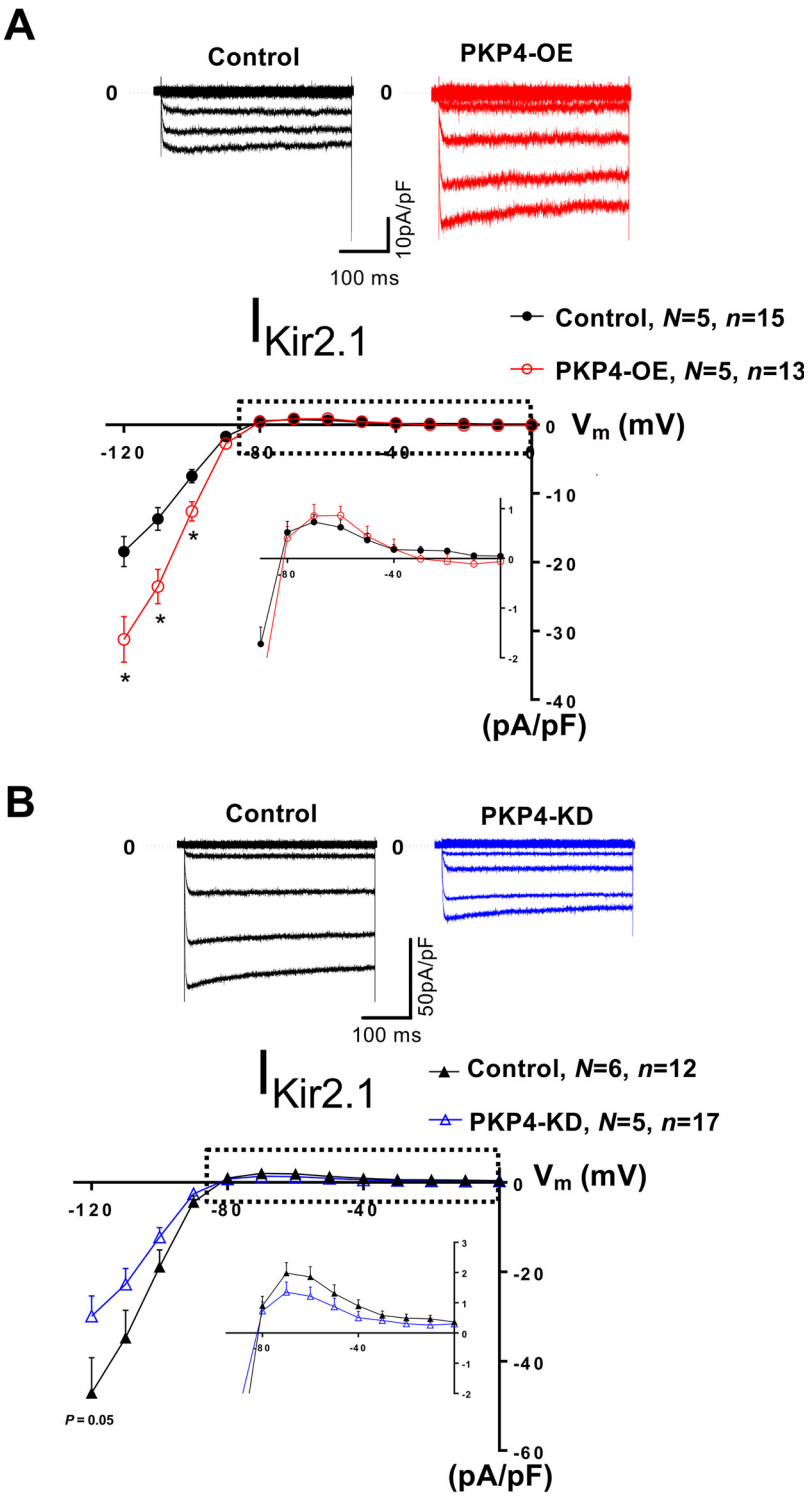


FIG. 5. **PKP4 is a positive regulator of $I_{Kir2.1}$.** Patch-clamping analyses in HEK293 cells upon genetic perturbation of *PKP4*, *i.e.* (*A*) upon overexpression of PKP4 and (*B*) upon CRISPR/Cas9-mediated depletion of PKP4. *$P < 0.05$ *versus* control. *N*: number of transfected cell batches; *n*: number of cells; OE: overexpression; $K_D$: knock-down.

proteins expressed in the heart, ARVC can be considered a disease of the desmosome (63). Mutations in the *JUP* genes have also been associated with Naxos disease, a diffuse nonepidermolytic palmoplantar keratoderma with wooly hair and cardiomyopathy (64). We also note that *JUP* mRNA is highly differentially expressed in AF (65).

*Functional Validation of PKP4 by Immunofluorescence and Patch-Clamp Analyses—PKP4* is one of the desmosome proteins identified in our BioID experiment as interacting with both Kir2.1$^{WT}$ and Kir2.1$^{\Delta 314\text{-}315}$ (normalized SpC counts: Kir2.1$^{WT}$: 23.3 and Kir2.1$^{\Delta 314\text{-}315}$: 7.6). PKP4 is a multifunctional armadillo protein coordinating cell adhesion with cytoskeletal organization that also has a role in vesicle transport processes (66). Though less frequent than the ones observed for the *JUP*, *DSG2* and *DSC2* genes, mutations in the *PKP4* gene have been observed in ARVC patients (31, 32). Similarly to many other Kir2.1 interactors (8), PKP4 carries a PDZ binding site at its carboxyl terminus. We hypothesize that the Kir2.1-PKP4 interaction contributes to the regulation of Kir2.1.

As a first step toward validating the role of PKP4 as a regulator of Kir2.1, we investigated the subcellular localization of both proteins by immunofluorescence (IF) staining in freshly isolated adult rat ventricular myocytes. We observed that Kir2.1 and PKP4 co-localize at intercalated disks and at z-disks near the cardiac sarcomeres (Pearson correlation coefficient = 0.85) (Fig. 4).

Finally, to assess the functional relevance of PKP4 to the modulation of $I_{Kir2.1}$, we performed patch-clamp in the voltage clamp configuration (12, 13, 15) in a stable HEK293 cell line expressing Kir2.1 upon genetic perturbation of PKP4 (Fig. 5). Upon PKP4 overexpression, we observed a gain of $I_{Kir2.1}$ density (Fig. 5*A*). Accordingly, upon CRISPR/Cas9-mediated depletion of PKP4, we observed a loss of $I_{Kir2.1}$ density (Fig. 5*B*). Therefore, in addition to interacting with Kir2.1 (Fig. 2) and to being mutated in an ARVC patients (31, 32), PKP4 is a positive regulator of $I_{Kir2.1}$ density.

## CONCLUSION

Evidence accumulated over the last 20 years strongly indicates that potassium channels function depends on a complex and dynamic ensemble of molecular events occurring in various organelles in the cell that help in the assembly and delivery of the right channel subunits to the right place in the cell membrane at the right time. Understanding such molecular events should help uncover novel insights into how channelosome proteins and accessory proteins participate in the control of cardiac excitability and the mechanisms of arrhythmias. Using a BioID proteomic approach, we have generated the most comprehensive Kir2.1 interactome map known to date with 218 high-confidence Kir2.1 BioID hits, the vast majority of which are novel putative Kir2.1 interactors. Moreover, our approach allowed us to identify novel proteins that interact preferentially with either Kir2.1$^{WT}$ or the ATS1 mutant Kir2.1$^{\Delta 314\text{-}315}$, thus uncovering novel molecular mechanisms underlying Kir2.1 function/dysfunction in ATS1. Our Kir2.1 interactome map represents a repository for numerous novel biological hypotheses. Using patch-clamping, we verified the functional relevance of one of our hits, PKP4, to the modulation of $I_{Kir2.1}$, thus providing a molecular mechanism by which PKP4 may be involved in ARVC. This result validates the power of our BioID interactome approach in identifying functionally relevant Kir2.1 interactors and modulators of $I_{Kir2.1}$.

## DATA AVAILABILITY

The MS raw data and Proteome Discoverer protein identification have been deposited to the ProteomeXchange Consortium via the PRIDE partner repository (26) with the data set identifier PXD011004.

*Acknowledgments*—We thank Drs. Anne Claude Gingras (The Lunenfeld-Tanenbaum Research Institute, University of Toronto, Canada) and Brian Raught (Princess Margaret Cancer Center, University of Toronto, Canada) for providing us with BioID reagents. We thank Dr. Robin Kunkel for her help with the cell illustration shown in Fig. 3. We thank Dr. M. Vidal and members of the CCSB (Harvard Medical School, Boston) for sharing the *PKP4* ORFeome clone.

*Funding and additional information*—This work was supported by the National Institutes of Health (NIH) through the National Heart, Lung, and Blood Institute (NHLBI) grant R01HL122352 awarded to J.J., as well as the National Institute of General Medical Sciences (NIGMS) grant R01GM094231 and the National Cancer Institute (NCI) grant U24CA210967 awarded to A.I.N. R.K. is supported by the NCI support grant P30CA046592 awarded to the University of Michigan Rogel Cancer Center. The content is solely the responsibility of the authors and does not necessarily represent the official views of the NIH.

*Author contributions*—J.F.R. and J.J. conceived and directed the project. S.S.P., J.Y., D.M., K.P.C., V.B. and A.I.N. designed and performed the BioID experiments. R.K. performed the interactome profiling and enrichment analyses. D.P.B. and G.G.S. designed and performed the patch-clamping and the IF analyses. J.F.R. wrote the manuscript, with contributions from other coauthors.

*Conflict of interest*—Authors declare no competing interests.

*Abbreviations*—The abbreviations used are: ACN, acetonitrile; AF, atrial fibrillation; ARVC, arrhythmogenic right ventricular cardiomyopathy; ATS1, type-1 Andersen-Tawil syndrome; BirA*, promiscuous biotin ligase; CTRL, control; DAP, dystrophin-associated proteins; DIC, differential interference contrast; ER, endoplasmic reticulum; EV, empty vector control; FDR, false discovery rate; $I_{Kir2.1}$, inward rectifier potassium current; IF, immunofluorescence; KD, knock-down; LC-MS/MS, liquid chromatography with tandem mass spectrometry; MAGUK, membrane-associated guanylate kinase; MS, mass spectrometry; NAC, nascent polypeptide-associated complex;

OE, overexpression; ORF, open reading frame; PEI, polyethylenimine; R, the normalized Kir2.1$^{WT/\Delta 314\text{-}315}$ SpC ratio; SAINT, significance analysis of interactome; SpC, spectral count; SRP, signal recognition particle; Tet, tetracycline; TM, transmembrane; TM-CTRL, transmembrane protein control; WB, western blot; WT, wild type.

Received April 2, 2020, Published, MCP Papers in Press, June 15, 2020, DOI 10.1074/mcp.RA120.002071

REFERENCES


1. Wang, Z., Yue, L., White, M., Pelletier, G., and Nattel, S. (1998) Differential distribution of inward rectifier potassium channel transcripts in human atrium versus ventricle. *Circulation* **98,** 2422–2428
2. Nichols, C. G., Makhina, E. N., Pearson, W. L., Sha, Q., and Lopatin, A. N. (1996) Inward rectification and implications for cardiac excitability. *Circ. Res*. **78,** 1–7
3. Hibino, H., Inanobe, A., Furutani, K., Murakami, S., Findlay, I., and Kurachi, Y. (2010) Inwardly rectifying potassium channels: their structure, function, and physiological roles. *Physiol. Rev*. **90,** 291–366
4. Plaster, N. M., Tawil, R., Tristani-Firouzi, M., Canún, S., Bendahhou, S., Tsunoda, A., Donaldson, M. R., Iannaccone, S. T., Brunt, E., Barohn, R., Clark, J., Deymeer, F., George, A. L., Fish, F. A., Hahn, A., Nitu, A., Ozdemir, C., Serdaroglu, P., Subramony, S. H., Wolfe, G., Fu, Y. H., and Ptácek, L. J. (2001) Mutations in Kir2.1 cause the developmental and episodic electrical phenotypes of Andersen's syndrome. *Cell* **105,** 511–519
5. Nguyen, H. L., Pieper, G. H., and Wilders, R. (2013) Andersen-Tawil syndrome: clinical and molecular aspects. *Int J Cardiol* **170,** 1–16
6. Priori, S. G., Pandit, S. V., Rivolta, I., Berenfeld, O., Ronchetti, E., Dhamoon, A., Napolitano, C., Anumonwo, J., di Barletta, M. R., Gudapakkam, S., Bosi, G., Stramba-Badiale, M., and Jalife, J. (2005) A novel form of short QT syndrome (SQT3) is caused by a mutation in the KCNJ2 gene. *Circ. Res*. **96,** 800–807
7. Abriel, H., Rougier, J. S., and Jalife, J. (2015) Ion channel macromolecular complexes in cardiomyocytes: roles in sudden cardiac death. *Circ. Res*. **116,** 1971–1988
8. Willis, B. C., Ponce-Balbuena, D., and Jalife, J. (2015) Protein assemblies of sodium and inward rectifier potassium channels control cardiac excitability and arrhythmogenesis. *Am. J. Physiol. Heart Circ Physiol* **308,** H1463–H1473
9. Leonoudakis, D., Conti, L. R., Radeke, C. M., McGuire, L. M., and Vandenberg, C. A. (2004) A multiprotein trafficking complex composed of SAP97, CASK, Veli, and Mint1 is associated with inward rectifier Kir2 potassium channels. *J. Biol. Chem*. **279,** 19051–19063
10. Leonoudakis, D., Mailliard, W., Wingerd, K., Clegg, D., and Vandenberg, C. (2001) Inward rectifier potassium channel Kir2.2 is associated with synapse-associated protein SAP97. *J. Cell Sci*. **114,** 987–998
11. Leonoudakis, D., Conti, L. R., Anderson, S., Radeke, C. M., McGuire, L. M., Adams, M. E., Froehner, S. C., Yates, J. R., 3rd, and Vandenberg, C. A. (2004) Protein trafficking and anchoring complexes revealed by proteomic analysis of inward rectifier potassium channel (Kir2.x)-associated proteins. *J. Biol. Chem*. **279,** 22331–22346
12. Milstein, M. L., Musa, H., Balbuena, D. P., Anumonwo, J. M., Auerbach, D. S., Furspan, P. B., Hou, L., Hu, B., Schumacher, S. M., Vaidyanathan, R., Martens, J. R., and Jalife, J. (2012) Dynamic reciprocity of sodium and potassium channel expression in a macromolecular complex controls cardiac excitability and arrhythmia. *Proc. Natl. Acad. Sci. U S A* **109,** E2134–E2143
13. Matamoros, M., Pérez-Hernández, M., Guerrero-Serna, G., Amorós, I., Barana, A., Núñez, M., Ponce-Balbuena, D., Sacristán, S., Gómez, R., Tamargo, J., Caballero, R., Jalife, J., and Delpón, E. (2016) Nav1.5 N-terminal domain binding to alpha1-syntrophin increases membrane density of human Kir2.1, Kir2.2 and Nav1.5 channels. *Cardiovasc. Res* .**110,** 279–290
14. Utrilla, R. G., Nieto-Marín, P., Alfayate, S., Tinaquero, D., Matamoros, M., Pérez-Hernández, M., Sacristán, S., Ondo, L., de Andrés, R., Díez-Guerra, F. J., Tamargo, J., Delpón, E., and Caballero, R. (2017) Kir2.1-Nav1.5 Channel Complexes Are Differently Regulated than Kir2.1 and Nav1.5 Channels Alone. *Front Physiol* **8,** 903
15. Ponce-Balbuena, D., Guerrero-Serna, G., Valdivia, C. R., Caballero, R., Diez-Guerra, F. J., Jiménez-Vázquez, E. N., Ramírez, R. J., Monteiro da Rocha, A., Herron, T. J., Campbell, K. F., Willis, B. C., Alvarado, F. J., Zarzoso, M., Kaur, K., Pérez-Hernández, M., Matamoros, M., Valdivia, H. H., Delpón, E., and Jalife, J. (2018) Cardiac Kir2.1 and NaV1.5 Channels Traffic Together to the Sarcolemma to Control Excitability. *Circ. Res*. **122,** 1501–1516
16. Li, P., Li, J., Wang, L., and Di, L. J. (2017) Proximity labeling of interacting proteins: Application of BioID as a discovery tool. *Proteomics* **17,** 1700002
17. Roux, K. J., Kim, D. I., Raida, M., and Burke, B. (2012) A promiscuous biotin ligase fusion protein identifies proximal and interacting proteins in mammalian cells. *J. Cell Biol*. **196,** 801–810
18. Lambert, J. P., Tucholska, M., Go, C., Knight, J. D., and Gingras, A. C. (2015) Proximity biotinylation and affinity purification are complementary approaches for the interactome mapping of chromatin-associated protein complexes. *J Proteomics* **118,** 81–94
19. Ma, D., Taneja, T. K., Hagen, B. M., Kim, B. Y., Ortega, B., Lederer, W. J., and Welling, P. A. (2011) Golgi export of the Kir2.1 channel is driven by a trafficking signal located within its tertiary structure. *Cell* **145,** 1102–1115
20. Bendahhou, S., Donaldson, M. R., Plaster, N. M., Tristani-Firouzi, M., Fu, Y.-H., and Ptácek, L. J. (2003) Defective potassium channel Kir2.1 trafficking underlies Andersen-Tawil syndrome. *J. Biol. Chem*. **278,** 51779–51785
21. Rual, J. F., Hirozane-Kishikawa, T., Hao, T., Bertin, N., Li, S., Dricot, A., Li, N., Rosenberg, J., Lamesch, P., Vidalain, P. O., Clingingsmith, T. R., Hartley, J. L., Esposito, D., Cheo, D., Moore, T., Simmons, B., Sequerra, R., Bosak, S., Doucette-Stamm, L., Le Peuch, C., Vandenhaute, J., Cusick, M. E., Albala, J. S., Hill, D. E., and Vidal, M. (2004) Human ORFeome version 1.1: a platform for reverse proteomics. *Genome Res*. **14,** 2128–2135
22. Xu, T., Park, S. S., Giaimo, B. D., Hall, D., Ferrante, F., Ho, D. M., Hori, K., Anhezini, L., Ertl, I., Bartkuhn, M., Zhang, H., Milon, E., Ha, K., Conlon, K. P., Kuick, R., Govindarajoo, B., Zhang, Y., Sun, Y., Dou, Y., Basrur, V., Elenitoba-Johnson, K. S., Nesvizhskii, A. I., Ceron, J., Lee, C. Y., Borggrefe, T., Kovall, R. A., and Rual, J. F. (2017) RBPJ/CBF1 interacts with L3MBTL3/MBT1 to promote repression of Notch signaling via histone demethylase KDM1A/LSD1. *EMBO J*. **36,** 3232–3249
23. Labun, K., Montague, T. G., Gagnon, J. A., Thyme, S. B., and Valen, E. (2016) CHOPCHOP v2: a web tool for the next generation of CRISPR genome engineering. *Nucleic Acids Res*. **44,** W272–W276
24. Ran, F. A., Hsu, P. D., Wright, J., Agarwala, V., Scott, D. A., and Zhang, F. (2013) Genome engineering using the CRISPR-Cas9 system. *Nat. Protoc*. **8,** 2281–2308
25. Longo, P. A., Kavran, J. M., Kim, M. S., and Leahy, D. J. (2013) Transient mammalian cell transfection with polyethylenimine (PEI). *Methods Enzymol*. **529,** 227–240
26. Deutsch, E. W., Csordas, A., Sun, Z., Jarnuczak, A., Perez-Riverol, Y., Ternent, T., Campbell, D. S., Bernal-Llinares, M., Okuda, S., Kawano, S., Moritz, R. L., Carver, J. J., Wang, M., Ishihama, Y., Bandeira, N., Hermjakob, H., and Vizcaíno, J. A. (2017) The ProteomeXchange consortium in 2017: supporting the cultural change in proteomics public data deposition. *Nucleic Acids Res*. **45,** D1100–D1106
27. Choi, H., Larsen, B., Lin, Z. Y., Breitkreutz, A., Mellacheruvu, D., Fermin, D., Qin, Z. S., Tyers, M., Gingras, A. C., and Nesvizhskii, A. I. (2011) SAINT: probabilistic scoring of affinity purification-mass spectrometry data. *Nat. Methods* **8,** 70–73
28. Mellacheruvu, D., Wright, Z., Couzens, A. L., Lambert, J. P., St-Denis, N. A., Li, T., Miteva, Y. V., Hauri, S., Sardiu, M. E., Low, T. Y., Halim, V. A., Bagshaw, R. D., Hubner, N. C., Al-Hakim, A., Bouchard, A., Faubert, D., Fermin, D., Dunham, W. H., Goudreault, M., Lin, Z. Y., Badillo, B. G., Pawson, T., Durocher, D., Coulombe, B., Aebersold, R., Superti-Furga, G., Colinge, J., Heck, A. J., Choi, H., Gstaiger, M., Mohammed, S., Cristea, I. M., Bennett, K. L., Washburn, M. P., Raught, B., Ewing, R. M., Gingras, A. C., and Nesvizhskii, A. I. (2013) The CRAPome: a contaminant repository for affinity purification-mass spectrometry data. *Nat. Methods* **10,** 730–736
29. Janssen, P. M., Hiranandani, N., Mays, T. A., and Rafael-Fortney, J. A. (2005) Utrophin deficiency worsens cardiac contractile dysfunction present in dystrophin-deficient mdx mice. *Am. J. Physiol. Heart Circ Physiol* **289,** H2373–H2378
30. Ward-Caviness, C. K., Neas, L. M., Blach, C., Haynes, C. S., LaRocque-Abramson, K., Grass, E., Dowdy, E., Devlin, R. B., Diaz-Sanchez, D., Cascio, W. E., Lynn Miranda, M., Gregory, S. G., Shah, S. H., Kraus, W. E., and Hauser, E. R. (2016) Genetic Variants in the Bone Morphogenic Protein

Gene Family Modify the Association between Residential Exposure to Traffic and Peripheral Arterial Disease. *PLoS ONE* **11,** e0152670

31. Gandjbakhch, E., Vite, A., Gary, F., Fressart, V., Donal, E., Simon, F., Hidden-Lucet, F., Komajda, M., Charron, P., and Villard, E. (2013) Screening of genes encoding junctional candidates in arrhythmogenic right ventricular cardiomyopathy/dysplasia. *Europace* **15,** 1522–1525
32. Xu, T., Yang, Z., Vatta, M., Rampazzo, A., Beffagna, G., Pilichou, K., Pillichou, K., Scherer, S. E., Saffitz, J., Kravitz, J., Zareba, W., Danieli, G. A., Lorenzon, A., Nava, A., Bauce, B., Thiene, G., Basso, C., Calkins, H., Gear, K., Marcus, F., and Towbin, J. A, Multidisciplinary Study of Right Ventricular Dysplasia Investigators, (2010) Compound and digenic heterozygosity contributes to arrhythmogenic right ventricular cardiomyopathy. *J. Am. Coll. Cardiol*. **55,** 587–597
33. Chatr-Aryamontri, A., Oughtred, R., Boucher, L., Rust, J., Chang, C., Kolas, N. K., O'Donnell, L., Oster, S., Theesfeld, C., Sellam, A., Stark, C., Breitkreutz, B. J., Dolinski, K., and Tyers, M. (2017) The BioGRID interaction database: 2017 update. *Nucleic Acids Res*. **45,** D369–D379
34. Orchard, S., Ammari, M., Aranda, B., Breuza, L., Briganti, L., Broackes-Carter, F., Campbell, N. H., Chavali, G., Chen, C., del-Toro, N., Duesbury, M., Dumousseau, M., Galeota, E., Hinz, U., Iannuccelli, M., Jagannathan, S., Jimenez, R., Khadake, J., Lagreid, A., Licata, L., Lovering, R. C., Meldal, B., Melidoni, A. N., Milagros, M., Peluso, D., Perfetto, L., Porras, P., Raghunath, A., Ricard-Blum, S., Roechert, B., Stutz, A., Tognolli, M., van Roey, K., Cesareni, G., and Hermjakob, H. (2014) The MIntAct project–IntAct as a common curation platform for 11 molecular interaction databases. *Nucleic Acids Res*. **42,** D358–D363
35. Keshava Prasad, T. S., Goel, R., Kandasamy, K., Keerthikumar, S., Kumar, S., Mathivanan, S., Telikicherla, D., Raju, R., Shafreen, B., Venugopal, A., Balakrishnan, L., Marimuthu, A., Banerjee, S., Somanathan, D. S., Sebastian, A., Rani, S., Ray, S., Harrys Kishore, C. J., Kanth, S., Ahmed, M., Kashyap, M. K., Mohmood, R., Ramachandra, Y. L., Krishna, V., Rahiman, B. A., Mohan, S., Ranganathan, P., Ramabadran, S., Chaerkady, R., and Pandey, A. (2009) Human Protein Reference Database–2009 update. *Nucleic Acids Res*. **37,** D767–D772
36. Rolland, T., Taşan, M., Charloteaux, B., Pevzner, S. J., Zhong, Q., Sahni, N., Yi, S., Lemmens, I., Fontanillo, C., Mosca, R., Kamburov, A., Ghiassian, S. D., Yang, X., Ghamsari, L., Balcha, D., Begg, B. E., Braun, P., Brehme, M., Broly, M. P., Carvunis, A.-R., Convery-Zupan, D., Corominas, R., Coulombe-Huntington, J., Dann, E., Dreze, M., Dricot, A., Fan, C., Franzosa, E., Gebreab, F., Gutierrez, B. J., Hardy, M. F., Jin, M., Kang, S., Kiros, R., Lin, G. N., Luck, K., MacWilliams, A., Menche, J., Murray, R. R., Palagi, A., Poulin, M. M., Rambout, X., Rasla, J., Reichert, P., Romero, V., Ruyssinck, E., Sahalie, J. M., Scholz, A., Shah, A. A., Sharma, A., Shen, Y., Spirohn, K., Tam, S., Tejeda, A. O., Trigg, S. A., Twizere, J.-C., Vega, K., Walsh, J., Cusick, M. E., Xia, Y., Barabási, A.-L., Iakoucheva, L. M., Aloy, P., De Las Rivas, J., Tavernier, J., Calderwood, M. A., Hill, D. E., Hao, T., Roth, F. P., and Vidal, M. (2014) A proteome-scale map of the human interactome network. *Cell* **159,** 1212–1226
37. Rual, J. F., Venkatesan, K., Hao, T., Hirozane-Kishikawa, T., Dricot, A., Li, N., Berriz, G. F., Gibbons, F. D., Dreze, M., Ayivi-Guedehoussou, N., Klitgord, N., Simon, C., Boxem, M., Milstein, S., Rosenberg, J., Goldberg, D. S., Zhang, L. V., Wong, S. L., Franklin, G., Li, S., Albala, J. S., Lim, J., Fraughton, C., Llamosas, E., Cevik, S., Bex, C., Lamesch, P., Sikorski, R. S., Vandenhaute, J., Zoghbi, H. Y., Smolyar, A., Bosak, S., Sequerra, R., Doucette-Stamm, L., Cusick, M. E., Hill, D. E., Roth, F. P., and Vidal, M. (2005) Towards a proteome-scale map of the human protein-protein interaction network. *Nature* **437,** 1173–1178
38. Braun, P., Tasan, M., Dreze, M., Barrios-Rodiles, M., Lemmens, I., Yu, H., Sahalie, J. M., Murray, R. R., Roncari, L., de Smet, A. S., Venkatesan, K., Rual, J. F., Vandenhaute, J., Cusick, M. E., Pawson, T., Hill, D. E., Tavernier, J., Wrana, J. L., Roth, F. P., and Vidal, M. (2009) An experimentally derived confidence score for binary protein-protein interactions. *Nat. Methods* **6,** 91–97
39. Huang da, W., Sherman, B. T., and Lempicki, R. A. (2009) Systematic and integrative analysis of large gene lists using DAVID bioinformatics resources. *Nat. Protoc*. **4,** 44–57
40. Kolb, A. R., Needham, P. G., Rothenberg, C., Guerriero, C. J., Welling, P. A., and Brodsky, J. L. (2014) ESCRT regulates surface expression of the Kir2.1 potassium channel. *Mol. Biol. Cell* **25,** 276–289
41. Tommasi di Vignano, A., Di Zenzo, G., Sudol, M., Cesareni, G., and Dente, L. (2000) Contribution of the different modules in the utrophin carboxy-terminal region to the formation and regulation of the DAP complex. *FEBS Lett*. **471,** 229–234
42. Matamoros, M., Pérez-Hernández, M., Guerrero-Serna, G., Amorós, I., Barana, A., Núñez, M., Ponce-Balbuena, D., Sacristán, S., Gómez, R., Tamargo, J., Caballero, R., Jalife, J., and Delpón, E. (2016) Nav1.5 N-terminal domain binding to alpha1-syntrophin increases membrane density of human Kir2.1 Kir2.2 and Nav1.5 channels. *Cardiovascular Research* **110,** 279–290
43. Rospert, S., Dubaquie, Y., and Gautschi, M. (2002) Nascent-polypeptide-associated complex. *Cell Mol Life Sci* **59,** 1632–1639
44. Yotov, W. V., and St-Arnaud, R. (1996) Differential splicing-in of a proline-rich exon converts alphaNAC into a muscle-specific transcription factor. *Genes Dev*. **10,** 1763–1772
45. Sims, R. J., 3rd, Weihe, E. K., Zhu, L., O'Malley, S., Harriss, J. V., and Gottlieb, P. D. (2002) m-Bop, a repressor protein essential for cardiogenesis, interacts with skNAC, a heart- and muscle-specific transcription factor. *J. Biol. Chem*. **277,** 26524–26529
46. Morales, J., Welter, D., Bowler, E. H., Cerezo, M., Harris, L. W., McMahon, A. C., Hall, P., Junkins, H. A., Milano, A., Hastings, E., Malangone, C., Buniello, A., Burdett, T., Flicek, P., Parkinson, H., Cunningham, F., Hindorff, L. A., and MacArthur, J. A. L. (2018) A standardized framework for representation of ancestry data in genomics studies, with application to the NHGRI-EBI GWAS Catalog. *Genome Biol.* **19,** 21
47. Roselli, C., Chaffin, M. D., Weng, L. C., Aeschbacher, S., Ahlberg, G., Albert, C. M., Almgren, P., Alonso, A., Anderson, C. D., Aragam, K. G., Arking, D. E., Barnard, J., Bartz, T. M., Benjamin, E. J., Bihlmeyer, N. A., Bis, J. C., Bloom, H. L., Boerwinkle, E., Bottinger, E. B., Brody, J. A., Calkins, H., Campbell, A., Cappola, T. P., Carlquist, J., Chasman, D. I., Chen, L. Y., Chen, Y. I., Choi, E. K., Choi, S. H., Christophersen, I. E., Chung, M. K., Cole, J. W., Conen, D., Cook, J., Crijns, H. J., Cutler, M. J., Damrauer, S. M., Daniels, B. R., Darbar, D., Delgado, G., Denny, J. C., Dichgans, M., Dorr, M., Dudink, E. A., Dudley, S. C., Esa, N., Esko, T., Eskola, M., Fatkin, D., Felix, S. B., Ford, I., Franco, O. H., Geelhoed, B., Grewal, R. P., Gudnason, V., Guo, X., Gupta, N., Gustafsson, S., Gutmann, R., Hamsten, A., Harris, T. B., Hayward, C., Heckbert, S. R., Hernesniemi, J., Hocking, L. J., Hofman, A., Horimoto, A., Huang, J., Huang, P. L., Huffman, J., Ingelsson, E., Ipek, E. G., Ito, K., Jimenez-Conde, J., Johnson, R., Jukema, J. W., Kaab, S., Kahonen, M., Kamatani, Y., Kane, J. P., Kastrati, A., Kathiresan, S., Katschnig-Winter, P., Kavousi, M., Kessler, T., Kietselaer, B. L., Kirchhof, P., Kleber, M. E., Knight, S., Krieger, J. E., Kubo, M., Launer, L. J., Laurikka, J., Lehtimaki, T., Leineweber, K., Lemaitre, R. N., Li, M., Lim, H. E., Lin, H. J., Lin, H., Lind, L., Lindgren, C. M., Lokki, M. L., London, B., Loos, R. J. F., Low, S. K., Lu, Y., Lyytikainen, L. P., Macfarlane, P. W., Magnusson, P. K., Mahajan, A., Malik, R., Mansur, A. J., Marcus, G. M., Margolin, L., Margulies, K. B., Marz, W., McManus, D. D., Melander, O., Mohanty, S., Montgomery, J. A., Morley, M. P., Morris, A. P., Muller-Nurasyid, M., Natale, A., Nazarian, S., Neumann, B., Newton-Cheh, C., Niemeijer, M. N., Nikus, K., Nilsson, P., Noordam, R., Oellers, H., Olesen, M. S., Orho-Melander, M., Padmanabhan, S., Pak, H. N., Pare, G., Pedersen, N. L., Pera, J., Pereira, A., Porteous, D., Psaty, B. M., Pulit, S. L., Pullinger, C. R., Rader, D. J., Refsgaard, L., Ribases, M., Ridker, P. M., Rienstra, M., Risch, L., Roden, D. M., Rosand, J., Rosenberg, M. A., Rost, N., Rotter, J. I., Saba, S., Sandhu, R. K., Schnabel, R. B., Schramm, K., Schunkert, H., Schurman, C., Scott, S. A., Seppala, I., Shaffer, C., Shah, S., Shalaby, A. A., Shim, J., Shoemaker, M. B., Siland, J. E., Sinisalo, J., Sinner, M. F., Slowik, A., Smith, A. V., Smith, B. H., Smith, J. G., Smith, J. D., Smith, N. L., Soliman, E. Z., Sotoodehnia, N., Stricker, B. H., Sun, A., Sun, H., Svendsen, J. H., Tanaka, T., Tanriverdi, K., Taylor, K. D., Teder-Laving, M., Teumer, A., Theriault, S., Trompet, S., Tucker, N. R., Tveit, A., Uitterlinden, A. G., Van Der Harst, P., Van Gelder, I. C., Van Wagoner, D. R., Verweij, N., Vlachopoulou, E., Volker, U., Wang, B., Weeke, P. E., Weijs, B., Weiss, R., Weiss, S., Wells, Q. S., Wiggins, K. L., Wong, J. A., Woo, D., Worrall, B. B., Yang, P. S., Yao, J., Yoneda, Z. T., Zeller, T., Zeng, L., Lubitz, S. A., Lunetta, K. L., and Ellinor, P. T. (2018) Multi-ethnic genome-wide association study for atrial fibrillation. *Nat. Genet*. **50,** 1225–1233
48. van der Harst, P., van Setten, J., Verweij, N., Vogler, G., Franke, L., Maurano, M. T., Wang, X., Mateo Leach, I., Eijgelsheim, M., Sotoodehnia, N., Hayward, C., Sorice, R., Meirelles, O., Lyytikainen, L. P., Polasek, O., Tanaka, T., Arking, D. E., Ulivi, S., Trompet, S., Muller-Nurasyid, M., Smith, A. V., Dorr, M., Kerr, K. F., Magnani, J. W., Del Greco, M. F., Zhang, W., Nolte, I. M., Silva, C. T., Padmanabhan, S., Tragante, V., Esko, T., Abecasis,

G. R., Adriaens, M. E., Andersen, K., Barnett, P., Bis, J. C., Bodmer, R., Buckley, B. M., Campbell, H., Cannon, M. V., Chakravarti, A., Chen, L. Y., Delitala, A., Devereux, R. B., Doevendans, P. A., Dominiczak, A. F., Ferrucci, L., Ford, I., Gieger, C., Harris, T. B., Haugen, E., Heinig, M., Hernandez, D. G., Hillege, H. L., Hirschhorn, J. N., Hofman, A., Hubner, N., Hwang, S. J., Iorio, A., Kahonen, M., Kellis, M., Kolcic, I., Kooner, I. K., Kooner, J. S., Kors, J. A., Lakatta, E. G., Lage, K., Launer, L. J., Levy, D., Lundby, A., Macfarlane, P. W., May, D., Meitinger, T., Metspalu, A., Nappo, S., Naitza, S., Neph, S., Nord, A. S., Nutile, T., Okin, P. M., Olsen, J. V., Oostra, B. A., Penninger, J. M., Pennacchio, L. A., Pers, T. H., Perz, S., Peters, A., Pinto, Y. M., Pfeufer, A., Pilia, M. G., Pramstaller, P. P., Prins, B. P., Raitakari, O. T., Raychaudhuri, S., Rice, K. M., Rossin, E. J., Rotter, J. I., Schafer, S., Schlessinger, D., Schmidt, C. O., Sehmi, J., Sillje, H. H. W., Sinagra, G., Sinner, M. F., Slowikowski, K., Soliman, E. Z., Spector, T. D., Spiering, W., Stamatoyannopoulos, J. A., Stolk, R. P., Strauch, K., Tan, S. T., Tarasov, K. V., Trinh, B., Uitterlinden, A. G., van den Boogaard, M., van Duijn, C. M., van Gilst, W. H., Viikari, J. S., Visscher, P. M., Vitart, V., Volker, U., Waldenberger, M., Weichenberger, C. X., Westra, H. J., Wijmenga, C., Wolffenbuttel, B. H., Yang, J., Bezzina, C. R., Munroe, P. B., Snieder, H., Wright, A. F., Rudan, I., Boyer, L. A., Asselbergs, F. W., van Veldhuisen, D. J., Stricker, B. H., Psaty, B. M., Ciullo, M., Sanna, S., Lehtimaki, T., Wilson, J. F., Bandinelli, S., Alonso, A., Gasparini, P., Jukema, J. W., Kaab, S., Gudnason, V., Felix, S. B., Heckbert, S. R., de Boer, R. A., Newton-Cheh, C., Hicks, A. A., Chambers, J. C., Jamshidi, Y., Visel, A., Christoffels, V. M., Isaacs, A., Samani, N. J., and de Bakker, P. I. W. (2016) 52 Genetic loci influencing myocardial mass. *J. Am. Coll. Cardiol*. **68,** 1435–1448

49. Li, H., Randall, W. R., and Du, S. J. (2009) skNAC (skeletal Naca), a muscle-specific isoform of Naca (nascent polypeptide-associated complex alpha), is required for myofibril organization. *Faseb J*. **23,** 1988–2000
50. Park, C. Y., Pierce, S. A., von Drehle, M., Ivey, K. N., Morgan, J. A., Blau, H. M., and Srivastava, D. (2010) skNAC, a Smyd1-interacting transcription factor, is involved in cardiac development and skeletal muscle growth and regeneration. *Proc. Natl. Acad. Sci. U S A* **107,** 20750–20755
51. Tristani-Firouzi, M., Jensen, J. L., Donaldson, M. R., Sansone, V., Meola, G., Hahn, A., Bendahhou, S., Kwiecinski, H., Fidzianska, A., Plaster, N., Fu, Y. H., Ptacek, L. J., and Tawil, R. (2002) Functional and clinical characterization of KCNJ2 mutations associated with LQT7 (Andersen syndrome). *J. Clin. Invest*. **110,** 381–388
52. Tawil, R., Ptacek, L. J., Pavlakis, S. G., DeVivo, D. C., Penn, A. S., Ozdemir, C., and Griggs, R. C. (1994) Andersen's syndrome: potassium-sensitive periodic paralysis, ventricular ectopy, and dysmorphic features. *Ann. Neurol*. **35,** 326–330
53. Yoon, G., Oberoi, S., Tristani-Firouzi, M., Etheridge, S. P., Quitania, L., Kramer, J. H., Miller, B. L., Fu, Y. H., and Ptácek, L. J. (2006) Andersen-Tawil syndrome: prospective cohort analysis and expansion of the phenotype. *Am. J. Med. Genet. A* **140,** 312–321
54. Tereshchenko, L. G., Sotoodehnia, N., Sitlani, C. M., Ashar, F. N., Kabir, M., Biggs, M. L., Morley, M. P., Waks, J. W., Soliman, E. Z., Buxton, A. E., Biering-Sorensen, T., Solomon, S. D., Post, W. S., Cappola, T. P., Siscovick, D. S., and Arking, D. E. (2018) Genome-Wide Associations of Global Electrical Heterogeneity ECG Phenotype: The ARIC (Atherosclerosis Risk in Communities) Study and CHS (Cardiovascular Health Study). *J. Am. Heart Assoc*. **7**
55. Wischmeyer, E., Doring, F., and Karschin, A. (1998) Acute suppression of inwardly rectifying Kir2.1 channels by direct tyrosine kinase phosphorylation. *J. Biol. Chem*. **273,** 34063–34068
56. Kutlu, B., Burdick, D., Baxter, D., Rasschaert, J., Flamez, D., Eizirik, D. L., Welsh, N., Goodman, N., and Hood, L. (2009) Detailed transcriptome atlas of the pancreatic beta cell. *BMC Med. Genomics* **2,** 3
57. Riz, M., Braun, M., Wu, X., and Pedersen, M. G. (2015) Inwardly rectifying Kir2.1 currents in human beta-cells control electrical activity: characterisation and mathematical modelling. *Biochem. Biophys. Res. Commun*. **459,** 284–287
58. Yildirim, V., Vadrevu, S., Thompson, B., Satin, L. S., and Bertram, R. (2017) Upregulation of an inward rectifying K+ channel can rescue slow Ca2+ oscillations in K(ATP) channel deficient pancreatic islets. *PLoS Comput. Biol*. **13,** e1005686
59. Kobayashi, S., Nagao, M., Asai, A., Fukuda, I., Oikawa, S., and Sugihara, H. (2018) Severity and multiplicity of microvascular complications are associated with QT interval prolongation in patients with type 2 diabetes. *J. Diabetes Investig*. **9,** 946–951
60. Veglio, M., Sivieri, R., Chinaglia, A., Scaglione, L., and Cavallo-Perin, P. (2000) QT interval prolongation and mortality in type 1 diabetic patients: a 5-year cohort prospective study. Neuropathy Study Group of the Italian Society of the Study of Diabetes, Piemonte Affiliate. *Diabetes Care* **23,** 1381–1383
61. Suys, B., Heuten, S., De Wolf, D., Verherstraeten, M., de Beeck, L. O., Matthys, D., Vrints, C., and Rooman, R. (2006) Glycemia and corrected QT interval prolongation in young type 1 diabetic patients: what is the relation? *Diabetes Care* **29,** 427–429
62. Torekov, S. S., Iepsen, E., Christiansen, M., Linneberg, A., Pedersen, O., Holst, J. J., Kanters, J. K., and Hansen, T. (2014) KCNQ1 long QT syndrome patients have hyperinsulinemia and symptomatic hypoglycemia. *Diabetes* **63,** 1315–1325
63. Swope, D., Li, J., and Radice, G. L. (2013) Beyond cell adhesion: the role of armadillo proteins in the heart. *Cell Signal*. **25,** 93–100
64. Cabral, R. M., Liu, L., Hogan, C., Dopping-Hepenstal, P. J. C., Winik, B. C., Asial, R. A., Dobson, R., Mein, C. A., Baselaga, P. A., Mellerio, J. E., Nanda, A., Boente, M. D C., Kelsell, D. P., McGrath, J. A., and South, A. P. (2010) Homozygous mutations in the 5' region of the JUP gene result in cutaneous disease but normal heart development in children. *J. Investigative Dermatol*. **130,** 1543–1550
65. Ou, F., Rao, N., Jiang, X., Qian, M., Feng, W., Yin, L., and Chen, X. (2013) Analysis on differential gene expression data for prediction of new biological features in permanent atrial fibrillation. *PLoS ONE* **8,** e76166
66. Keil, R., Schulz, J., and Hatzfeld, M. (2013) p0071/PKP4, a multifunctional protein coordinating cell adhesion with cytoskeletal organization. *Biol. Chem*. **394,** 1005–1017